AD 268 173

ASD TECHNICAL NOTE 61-65

CABLE AND PISTON DRAG PARAMETER INVESTIGATION FOR HYDRAULIC AIRCRAFT-ARRESTING ENERGY ABSORBERS

HOWARD L. PETERSON

RESEARCH, INCORPORATED

JUNE 1961

AEROSPACE GROUND EQUIPMENT ENGINEERING DIVISION

CONTRACT NR. AF 33(600)-40364
PROJECT NR. 6073
TASK NR. 60769

62-1-5
NOX

AERONAUTICAL SYSTEMS DIVISION
AIR FORCE SYSTEMS COMMAND
UNITED STATES AIR FORCE
WRIGHT-PATTERSON AIR FORCE BASE, OHIO

FOREWORD

This report was prepared by Research, Incorporated of Minneapolis Minnesota. It was written by Mr. H. L. Peterson. The investigation was conducted under contract AF 33(600)-40364 with Wright Air Development Division,* Aerospace Ground Equipment Engineering Division under the direction of Lt. Lassiter, Project engineer and Mr. V. V. Vary, Assistant Chief of Base Equipment Branch. At Research, Incorporated the program was directed by Mr. V. H. Larson as project engineer. In addition to the author, Messrs. H. R. Meline and R. W. Kreitz actively participated in the tests and analyses.

*Presently designated Aeronautical Systems Division

ABSTRACT

An investigation was conducted to obtain information on the parameters affecting operation or control of hydraulic energy asborbers used in barrier systems. The influence of independent variables on cable drag was investigated by pulling a test cable (wire rope) through a water filled tube at velocities up to 200 feet per second. Drag forces and tube water pressures were recorded for various test configurations. The variables included water tube length and diameter, smooth and rough test cable and varying amounts of water bleed. Results were analyzed and compared with full scale barrier tests.

The variation of piston drag with tube diameter was also investigated. Results, using both single and double piston arrangement were also compared to the full scale barrier tests.

PUBLICATION REVIEW

This report has been reviewed and is approved.

FOR THE COMMANDER:

W. A. ROSE
Chief, Base Equipment Branch
Aerospace Ground Eqp Engr Div
Deputy for Systems Engineering

TABLE OF CONTENTS

LIST OF APPENDICES

LIST OF ILLUSTRATIONS

LIST OF TABLES

INTRODUCTION

The Air Force has supported extensive developmental work on runway overrun barriers. The energy absorber barrier component has been the subject of several separate investigations. The hydraulic type energy absorber in particular has undergone broad test programs. The basic drag parameters, however, have not been defined sufficiently to augment further development. The purpose of this report is to present the results of an investigation to determine the relationship of cable and piston drag coefficients with the independent water tube design parameters. The application of these results should be useful not only to improve performance of present hydraulic energy absorbers, but should also provide basic information for the design of future installations.

Manuscript released by the author 15 February 1961 for publication as an ASD Technical Note.

SECTION I

FACILITY AND TEST EQUIPMENT

The Research, Incorporated test facility was designed and constructed under the current Air Force contract AF 33(600)-40364. The test facility is basically a pneumatically powered sled system guided by a monorail track with a total sled travel of approximately three hundred feet. The test site, located near the Company's main plant and facilities, utilizes a tract one thousand feet long with a maximum width of two hundred feet. The purpose of the test facility, in addition to the cable drag study covered in this report, is to provide adequate simulation of aircraft landing velocities and energies thus providing an inexpensive means to test prototype energy absorber system components.

A. Propulsion System

A basic concept in the design of the test facility was to use high pressure air to develop the high accelerating and sustaining forces required. In the design, propulsion was accomplished by porting high pressure air behind a floating piston housed in a 310 foot long cylinder. Energy was transmitted to test systems by attaching a one inch diameter wire rope to the floating piston. The power cylinder shown in the foreground of the photograph, figure 1, was constructed using tube sections with "O" ring sealed slip-over couplings. Tension rods held the tubes in their axial position and also maintained the position of the coupling through a connecting ring. Figure 2 shows the piston, cable and cable seal prior to insertion into the power cylinder. The photograph also shows how the high pressure air was ported into the cylinder. The connecting valve housings are shown prior to installation of the valve assembly. The valves developed by Research, Incorporated under a previous Air Force Contract will operate at pressures up to 15000 psi. At this maximum pressure, the propulsion system with a 7-1/4 inch diameter piston will provide an initial accelerating force of nearly 60,000 pounds.

B. Sled and Monorail Section

The sled and 300 foot long monorail section is part of the basic test facility. Their use in the cable drag investigation was primarily to serve as an intermediate link to pull the test cable. An emergency stop cable was positioned across the monorail track so that the sled would engage when 50 feet of travel remained. Figure 3 shows the sled after a low velocity

engagement with the emergency stop cable. The main pulling cable (power cable) as well as the trailing test cable were guided by a "U" shaped channel welded to the top of the I-beam monorail and are also shown in the photograph.

C. Deceleration Control and System Retrieve

Deceleration control was required to arrest the system after the test cable reached the desired velocity. Excellent control of the braking force was obtained by employing a hydraulic friction brake on the trailing length of the test cable. The brake shown in figure 4 was designed by Research, Incorporated and used for tests under a previous Air Force program. The brake was activated when the sled reached a specified position on the monorail track. The brake shoes were made from cast iron and were water cooled to improve their performance. The test cable behind the brake was enclosed in a pipe to restrain the cable during braking. Several unions were used to connect the pipe so that the trailing end of the test cable was accessible after a test run. A small electric winch was used to retrieve the system by attaching the winch cable to the test cable. The test cable was then threaded through the pipe after the sled, power cable and piston were retrieved.

D. Test Section

The test section for the cable drag investigation occupied a one hundred foot length between the end of the track and the hydraulic brake. Within this section the geometry was changed systematically during the test program. The basic test configuration was an 87 foot water-filled tube section. Labyrinth seals on each end of the tube allowed the test cable to be pulled through the tube with small seal friction. Assuming that the seal friction is negligible, the cable drag is then equal to the tube reaction force. The tube reaction force, hereafter called cable drag, was measured by mounting the tube on flexure supports and resisting the end load with a strain gage type load cell. Figure 5 shows the test section looking downstream from the hydraulic brake.

1. Test Section Geometry For Cable Drag Tests

Figure 6 illustrates the test section components showing a typical configuration with the variables noted. Design of the test section was given special consideration in order to permit configuration changes with a minimum of down time. Four lengths of extra strong (schedule 80) four inch pipe were used to build up the 87 foot long water tube. Both ends of the pipe sections were threaded, thus length changes were accomplished by joining

the desired number of pipe sections with standard couplings. The piovt frame and bulkhead were fabricated so that the load cell could be mounted in either of two positions; this increased the range of force measuring capability. Figure 7 shows the pivot assembly with the load cell mounted to measure the forces directly. The transducer for measuring tube water pressure is also shown mounted to the forged steel cross of the pivot assembly. Provisions for externally pressurizing the fluid cell were incorporated for calibration purposes.

The bleed orifice diameter was varied by installing a selected orifice plate. The plate was mounted on a modified pipe cap using an "O" ring seal. Figure 8 illustrates this assembly. A stand pipe was provided upstream from the orifice to properly straighten the orifice water flow. The upstream end of the water tube was connected to a water reservoir to keep the tube full during bleed operation. The reservoir was supported by the water tube in order that tube length changes might be conveniently made and also to eliminate intereference effects during the drag measurements.

The water tube diameter was reduced by inserting a two inch tube inside of the mounted four inch tube. The downstream end was welded to an adapter coupling which transmitted the forces to the four inch tube as well as providing a pressure seal. Ring spacers were attached to the small tube so that the original four inch tube not only supported the smaller tube but maintained the alignment as well.

2. Test Section Geometry For Piston Drag

The basic test section described above was modified in order to determine the effects of tube diameter on piston drag. The independent study of cable drag was assumed to produce sufficient information so that pure cable drag could be separated with sufficient accuracy from the total piston plus cable drag. A hydraulic energy absorber was constructed using tube sections varying from 6.25 inches in diameter at the retrieve end to 4.75 inches at the arrest end. A conical aluminum piston, 4.48 inches in diameter was attached to an identical 5/8 inch cable used in the cable drag tests. Test velocities could then be kept comparatively low to simulate operation in the smaller tube sections of the full scale "water squeezer". A consideration also in the selection of the tube diameters was that for a given piston diameter, the effects of tube diameter would be more pronounced in the smaller tube sections.

Figure 9 gives the tube dimensions used in the construction of the 225 foot long water squeezer; the figure also illustrates how this installation was

incorporated into the original cable drag test section. The water squeezer was mounted on flexure supports with approximately five foot spacing. Mounting by this method gave necessary support to the water tube and permitted only longitudinal deflection. The arrest end of the water squeezer was connected to the pivot frame through a transition coupling so that the tube pressures and reaction forces were measured in the same manner as with the pure cable drag tests.

3. Test Instrumentation

The test instrumentation for the drag investigation embodied primarily three components. A strain gage type load cell feeding into a full bridge circuit of a four channel Sanborn recording galvanometer gave a continuous measurement of cable drag. The second component measured the water pressure in the downstream end of the tube by means of a strain gage type pressure transducer, also connected to the recording galvanometer. The other principle component was a system of knock-out shunts, tripped by the sled at ten foot intervals which gave a trace of position versus time on a third channel of the recorder. The photograph, figure 10, shows the recorder on the left. An interconnection to the fire control panel (center) starts the recorder in advance of firing the propulsion control valves. The valves and gages pictured on the right provide pressurization controls for the propulsion valves and distribution control to other facility air systems from the main storage tanks.

FIGURE 1: ARRESTING GEAR TEST FACILITY

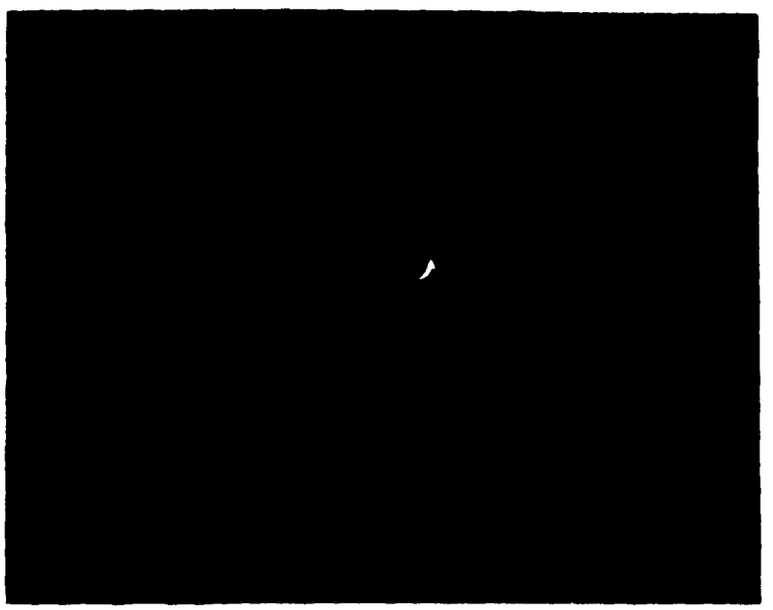

FIGURE 2: POWER PISTON ASSEMBLY

FIGURE 3: SLED AND MONORAIL TRACK SECTION

FIGURE 4: HYDRAULIC FRICTION BRAKE

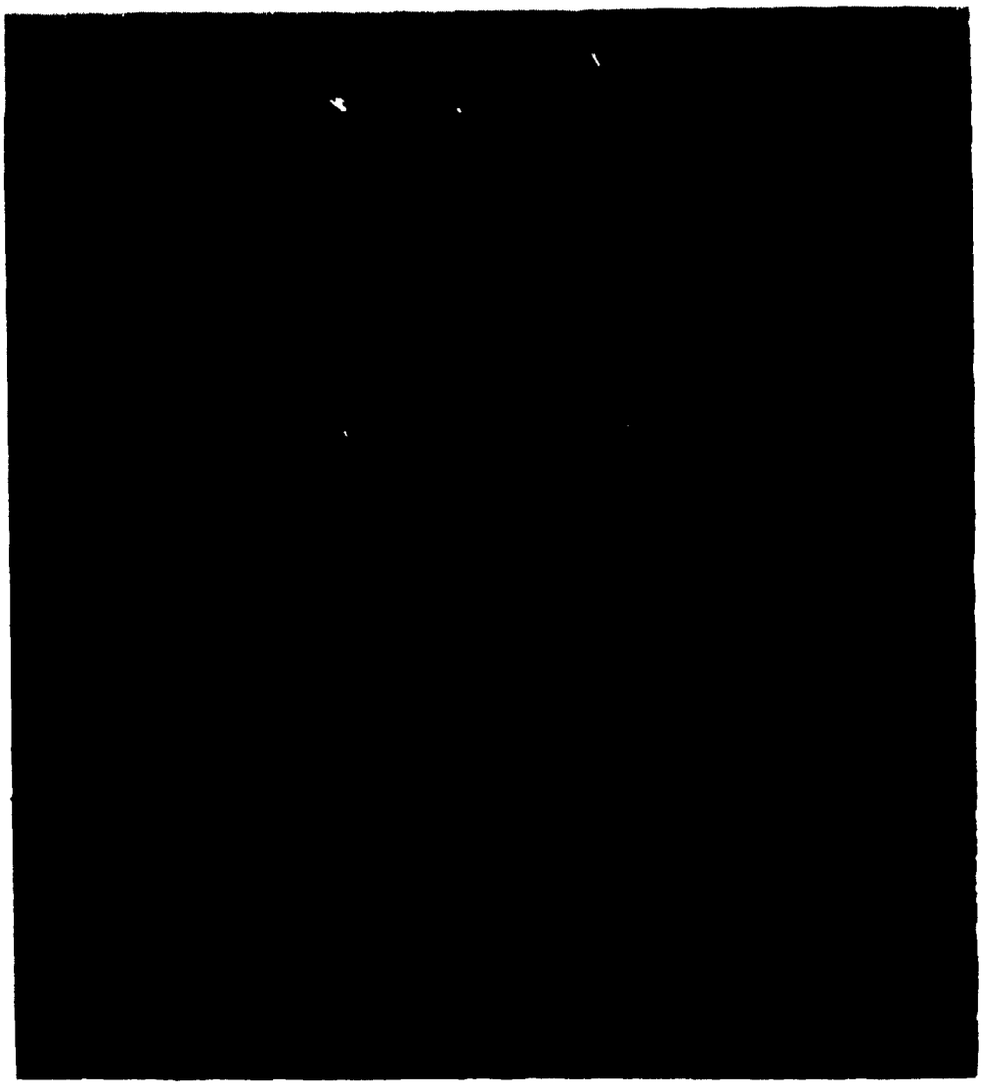

FIGURE 5: TEST SECTION - CABLE DRAG INVESTIGATION

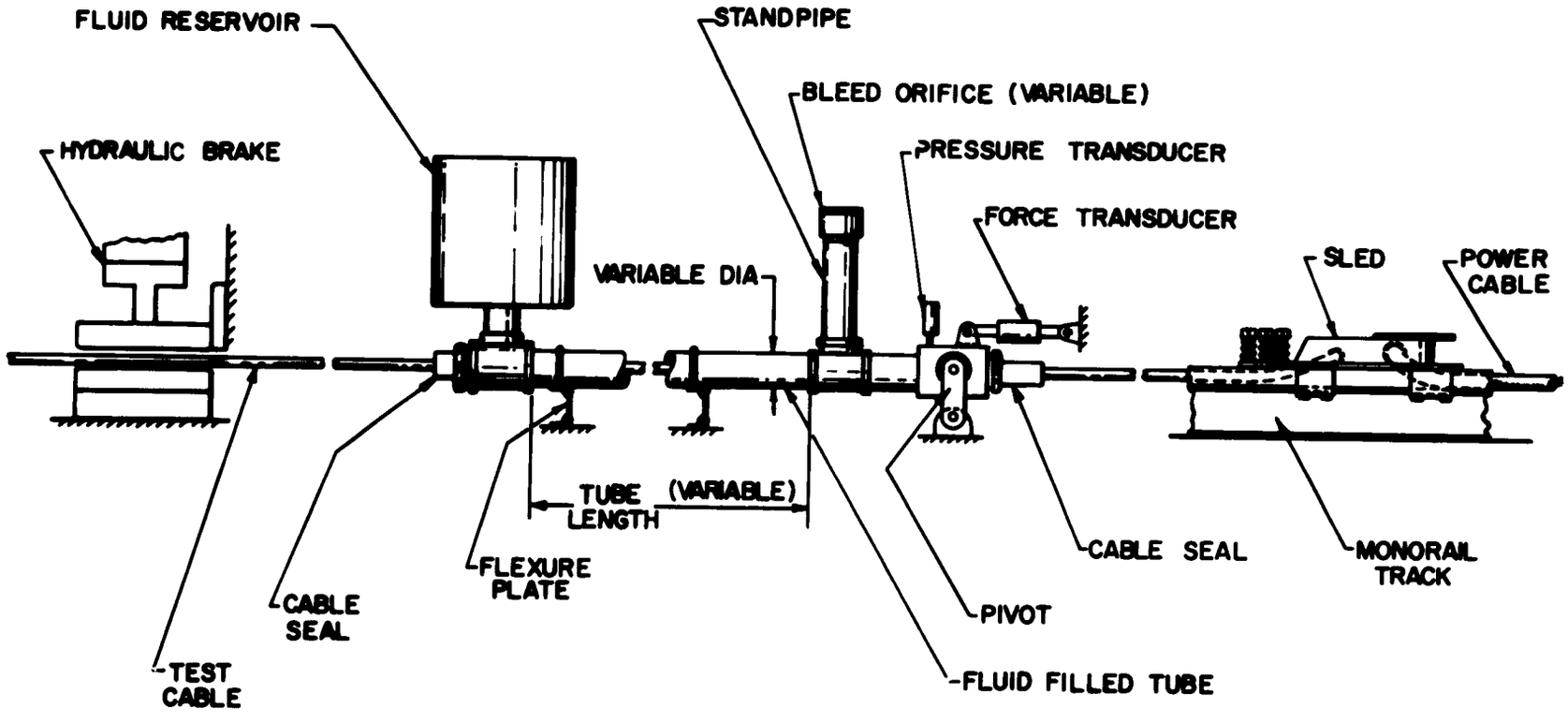

FIGURE 6: ILLUSTRATION OF CABLE DRAG TEST SECTION COMPONENTS

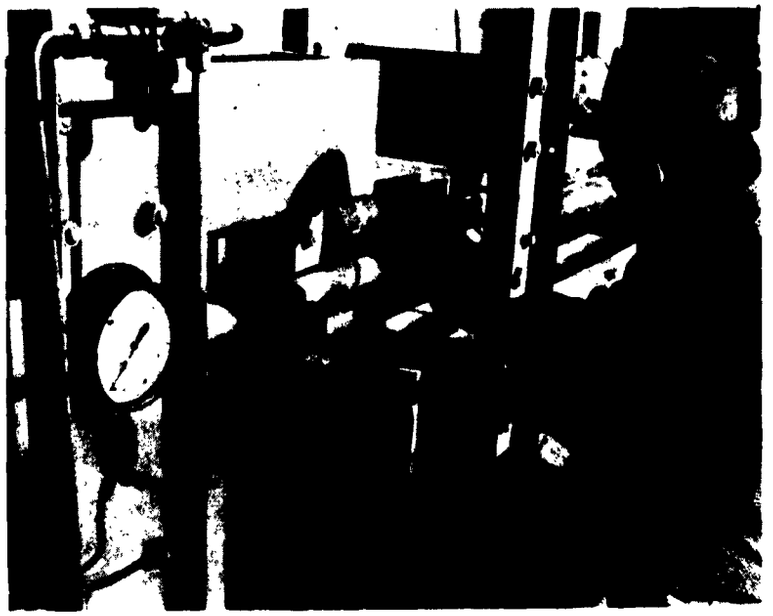

FIGURE 7: PIVOT ASSEMBLY WITH INSTRUMENTATION

FIGURE 8: STANDPIPE AND ORIFICE ASSEMBLY

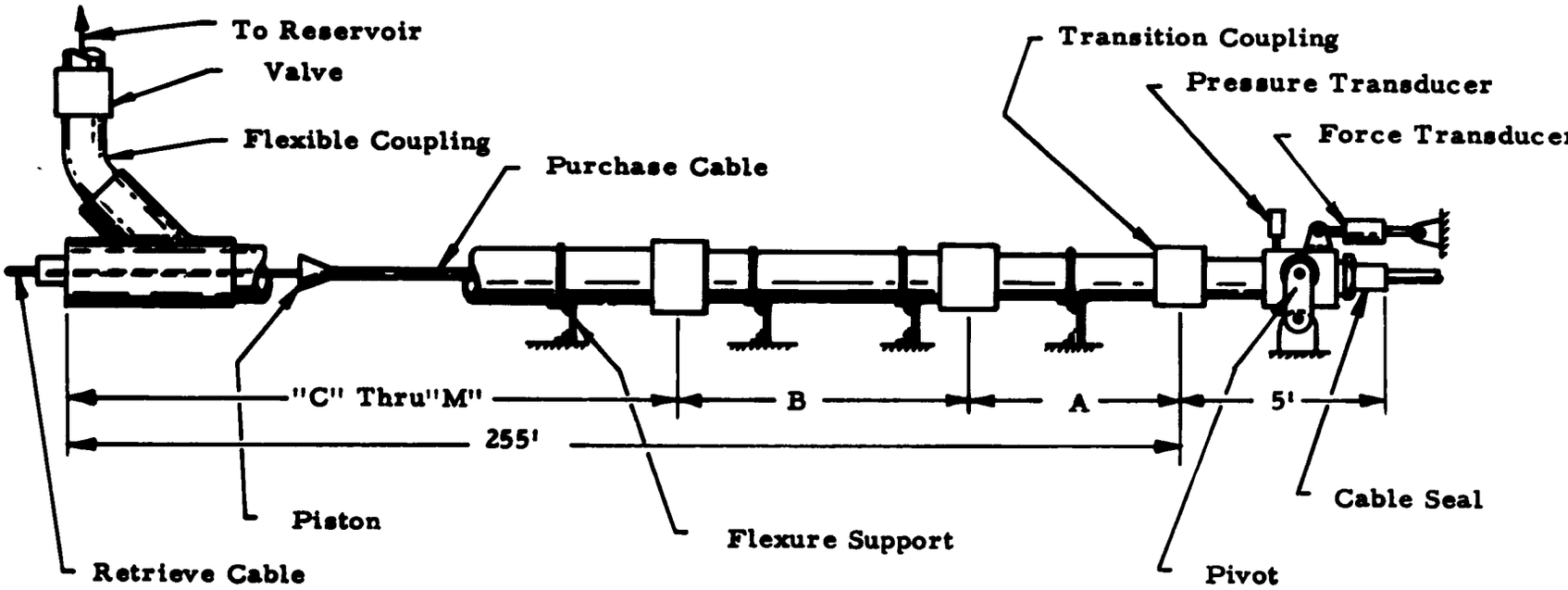

Tube Section	Tube Diameter, in.	Section Length, ft.
A	4.750	30
B	4.875	30
C	5.000	30
D	5.125	30
E	5.250	15
F	5.375	15
G	5.500	15

Tube Section	Tube Diameter, in.	Section Length, ft.
H	5.626	15
I	5.750	10
J	5.875	10
K	6.000	10
L	6.125	30
M	6.250	15

FIGURE 9: ILLUSTRATION OF PISTON DRAG TEST INSTALLATION

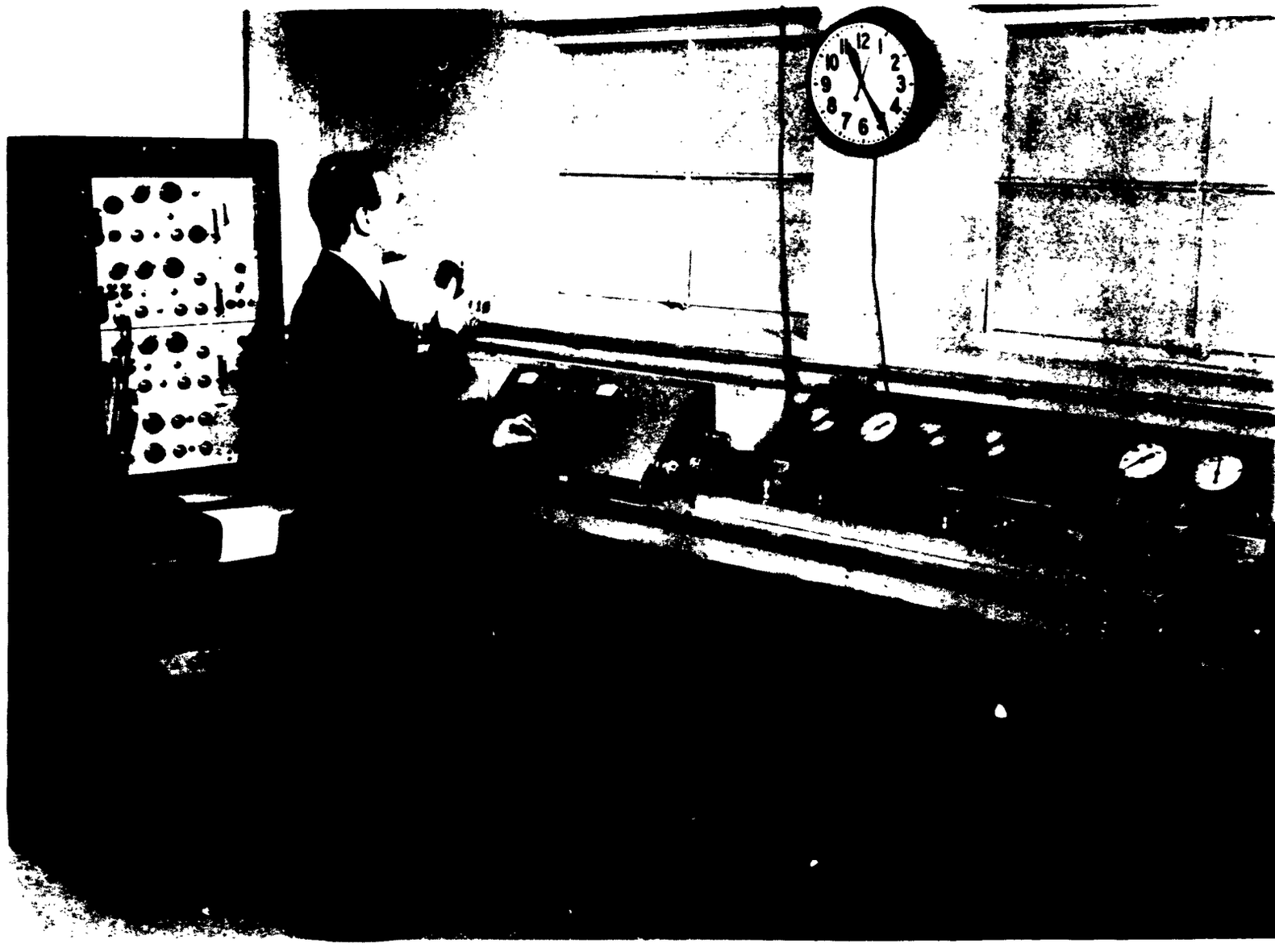

FIGURE 10: TEST CONTROL EQUIPMENT

SECTION II

TEST PROGRAM PROCEDURE

The test variables in the investigation of cable drag were water tube length and diameter, bleed orifice diameter, cable type and cable velocity. Table I lists the run numbers for the various test configurations. Test data results are tabulated according to run number and are presented in Table II. The cable drag coefficient in this tabulation was calculated from

$$C_D = \frac{D_c}{\frac{\rho}{2} A_c \ V_c^2} \tag{1}$$

where D_c = measured tube thrust minus tare forces, lbs

ρ = water density, lbs sec^2/ft^4

A_c = cable surface area equals $\left(\frac{\pi \ d \ c}{12}\right) L_T$, ft^2

$d\ c$ = cable diameter, in.

L_T = wetted length, ft

V_c = cable velocity, ft/sec

Data for each test configuration were taken at several maximum velocity conditions in order to minimize the acceleration effects of the cable. Figure 11 is a tracing of typical test run data. The constant chart speed of the recorder allows determinations of average velocity for each of the ten foot intervals. These velocity points are then plotted on the same time base to correlate velocity with the pressure and force measurements.

Table II also contains a tabulation of the data from the piston drag tests. These tests were conducted to obtain the variation of piston drag with tube diameter for a particular sized piston. Tests were also run using two pistons spaced at 25 feet to determine the added piston drag. A flow coefficient, C_e, was calculated for these tests from the following equation

$$C_e = \sqrt{\frac{V_c^2}{F_p} \quad K_p^2} \tag{2}$$

where F_p = measured tube thrust, F_m, minus cable drag, D_c, lbs

$K_p^2 = A_p\left(\frac{A_T}{A_f}\right)^2 \left[\, 1 - \left(\frac{A_f}{A_T}\right)^2 \,\right]$, ft^2

A_p = piston frontal area, equals 0.1096 ft^2

A_T = tube area, ft^2

A_f = flow area, equals $(A_T - A_p)$

$1-\left(\frac{A_f}{A_T}\right)^2$ = velocity of approach correction

Note: For the double piston combination, an average value of A_f/A_T was used since pistons were separated, and data points were not available where both pistons would lie in some tube section. $(A_f/A_T)_{avg}$ was calculated from

$$\left(\frac{A_f}{A_T}\right)_{avg} = \sqrt{\frac{\left(\frac{A_{f_1}}{A_{T_1}}\right)^2 + \left(\frac{A_{f_2}}{A_{T_2}}\right)^2}{2}} \qquad (3)$$

TEST CONFIGURATION												RUN NUMBER					
CABLE		TUBE LENGTH, FT			TUBE DIA, IN.		ORIFICE DIAMETER, IN.					CABLE VELOCITY RANGE, fps					
STANDARD	ARMOURED	25.5	46.5	89.5	1.94	3.83	0	.50	1.00	2.00	3.8	50-75	75-100	100-125	125-150	150-175	175-200
X				X		X	X					35	38	37	29	49	39
X				X		X	X					36				50	48
	X			X		X	X					51	52	53	54		
X				X		X		X				40			32	47	46
X				X		X			X			41			33		45
X				X		X				X		42			34		44
X				X		X					X			56			
X			X				X					57		59	60	61	
X			X						X								62
X		X					X					63	64		65	66	
X		X								X							67
X				X	X		X					68	69		70	74	
X				X	X			X							71		
X				X	X				X						72		
X				X	X					X					73		

TABLE I: TEST CONFIGURATIONS AND RUN NUMBERS FOR CABLE DRAG INVESTIGATION

RUN NO.	MAXIMUM VELOCITY ft/sec	TUBE PRESSURE psig	TUBE THRUST lb	DRAG COEFF.	REMARKS
27	152	---	---	---	Water hammer from air in standpipe
28	---	128	1400	---	Part of velocity trace missed
29	147	115	1320	.0041	
30	---	137	1600	---	Velocity questionable
31	176	175	1700	---	Force trace zero drift
32	155	130	1490	.0042	
33	155	118	1400	.0039	
34	158	61	1040	.0028	
35	64	20	230	.0038	
36	62	18.7	205	.0036	
37	118	---	850	.0042	Pressure trace off scale
38	88	42.5	480	.0042	
39	190	202	2230	.0042	
40	67	15	256	.0039	
41	66	13	215	.0033	
42	66	6	157	.0025	
43	68	0	---	---	Dry run -- forces negligible
44	200	78	1680	.0028	
45	197	146	2150	.0037	
46	195	---	2200	.0039	Pressure trace questionable
47	180	174	2000	.0042	
48	210	220	2500	.0039	
49	153	---	1430	.0041	Pressure trace questionable
50	163	145	1650	.0042	
51	99	9.7	166	.0022	
52	78	18.2	322	.0023	
53	113	40.7	645	.0024	
54	129	57	875	.0026	
55	63	15.8	280	.0024	
56	117	5.8	490	.0024	Open stand pipe bleed
57	58	9.7	115	.0044	

TABLE II: TABULATION OF TEST DATA AND CALCULATED DRAG COEFFICIENT

RUN NO.	MAXIMUM VELOCITY ft/sec	TUBE PRESSURE psig	TUBE THRUST lb	DRAG COEFF.	REMARKS
58	122	47	550	---	Brake failed; cable overtook sled
59	123	48	575	.0047	
60	143	58	750	.0042	
61	172	86	1100	.0043	
62	180	85	1020	.0037	Pressure trace questionable
63	70	6.8	78	.0038	
64	89	11.3	150	.0039	
65	121	21	290	.0039	
66	164	40.2	560	.0042	
67	165	32	495	.0034	
68	63	100	275	.0047	
69	84	160	480	.0046	
70	128	350	1130	.0047	
71	132	325	980	.0038	
72	135	167	725	.0027	
73	137	15	540	.0019	
74	148	465	1500	.0046	

RUN NO.	MAXIMUM VELOCITY ft/sec	MAX. TUBE PRESSURE psig	MAX. TUBE THRUST lb	PISTON CONFIGURATION	REMARKS
81	87	400	6,000	$4\frac{1}{2}$ in. O.D. Conical Aluminum (AAE type)	Retrieve end of water squeezer closed off
82	63	260	4,000		
83	105	700	10,000		
84	110	900	11,500		
85	130	1050	21,000		
86	130	1000	20,000		Pressure relief valve installed in retrieve end of water squeezer
87	88	480	9,000		
88	90	600	9,000	Double Pistons (same as above)	
89	90	600	9,000		Valve closed downstream of relief valve
90	108	750	10,000		
91	73	440	6,000		

TABLE II (cont): TABULATION OF TEST DATA AND CALCULATED DRAG COEFFICIENT

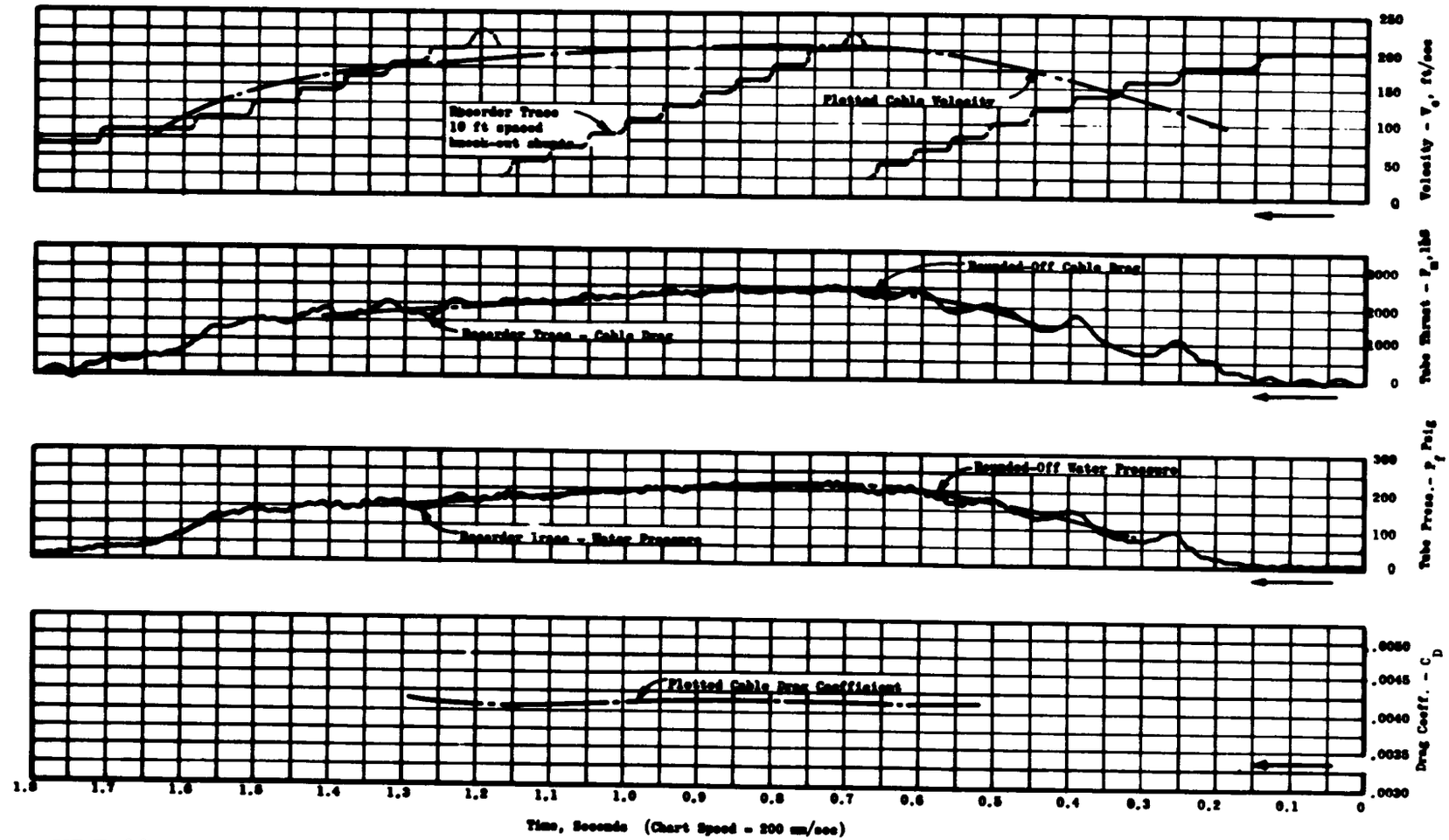

FIGURE 11: TYPICAL TRACED COPY OF RECORDED AND PLOTTED CABLE DRAG DATA (Run No. 48)

SECTION III

RESULTS AND DISCUSSION

Cable drag tests were conducted for a number of different configurations to evaluate the primary effects of tube length, tube diameter, cable roughness and water bleed. In this evaluation it was necessary to determine the effect of the cable seal for each configuration. A labyrinth type seal was used with approximately 0.060 clearance on the diameter. This amount of clearance was deemed necessary to minimize binding of the cable in the seal while tensioning and relaxing during a test run. It was also assumed that the pressure measured in the downstream end of the tube would only be slightly affected by pressure loss through the seal. Tests on the longest four inch tube substantiated these assumptions by showing that the measured pressure multiplied by the tube cross-sectional area was essentially equal to the measured tube reaction force during zero bleed operation. This correlation would not hold, certainly, for high bleed operation since the viscous shear energy derived from the cable travel is partially used to pump water through the orifice. The difference for zero bleed then, between the calculated tube thrust and the measured thrust must be considered as tare drag. One exception to this was for the case of "zero" bleed operation with the two inch diameter water tube. The seal clearance plus the voids in the standard cable amount to a flow area equivalent to a bleed orifice diameter of 0.4 inch which is enough to produce a significant effect on the measured thrust. At the higher pressures produced with this configuration, the bleed would probably be significantly greater than zero.

A. Cable Geometry

The effect of cable geometry on the cable drag was demonstrated by comparing test results of a 1/2 inch armoured cable with a 5/8 inch 7 x 19 left lay cable; figure 12 is a photograph of the test cables used. The measured diameters were used as the basis for computing drag coefficient and were nearly equal, 0.658 and 0.652 inches, respectively. The results shown as figure 13 indicate that a 40 percent reduction in drag coefficient was realized by the use of a comparatively smooth surfaced cable in place of a standard lay cable. The marked change in drag due to surface roughness was compared with pipe flow data using an analogy explained in Appendix I. This approximation shows that the standard lay cable has an absolute roughness, equal to 0.0120 feet, and the armoured cable, $e = 0.0011$ feet. These calculated values are plotted in figure 14 showing the surface roughness of other materials for comparison.

The practical use of an armoured purchase cable would depend on its dynamic characteristics as well as its drag alleviation qualities. In drag reduction, armoured cable would reduce total drag only by about 20 percent since the armour would increase the diameter for an equivalent strength cable.

B. Tube Diameter

The effect of the water tube diameter on the cable drag coefficient must necessarily be a function of the relative diameter of cable with respect to the tube diameter. In this investigation a four inch water tube with a 5/8 inch cable was selected as being comparable with present hydraulic energy absorber water tube and cable dimensions. The tube diameter was then reduced by a factor of two so that differences in the test results would be more evident. The results from this test series with the smaller water tube showed an increase in the drag coefficient of approximately 13 percent (figure 15). By taking into account the effective bleeding through the cable seal, the tru zero bleed difference becomes 20 percent. The curves of figure 17 give the drag coefficient values of 0.0042 for the 3.83 inch diameter tube and 0.0051 for the 1.94 inch diameter tube. The increased drag with the reduced tube diameter points out that the reverse flow became significant with the small tube, and the test cable felt this as an increased relative velocity - hence higher shear forces. The reverse flow velocity in the water tube is a function of the cross-sectional area, therefore one would expect small reduction in drag coefficient by increasing the tube diameter beyond four inches.

C. Tube Length

The effect of tube length on the cable drag coefficient was demonstrated by tests on tubes of one-half and one-fourth of the original 89.5 feet. The results plotted in figure 16 show very little change in the drag coefficient. The tare drag in the system was more pronounced with the short lengths, as indicated by comparing the measured force with the calculated reaction force based on the measured pressure.

Oscillograph data from full scale hydraulic energy absorber tests at Edwards Air Force Base were analyzed to obtain comparative results. The cable drag coefficient was determined from this data by considering pressures, velocities and cable tensions before the pistons entered the water filled sections of tube. The analysis of a typical test run is given in Appendix II to show the compatibility of the measured pressures with the assumed distribution

The cable drag coefficient from this analysis as calculated was 0.0036. From figure 18 the predicted drag coefficient is 0.0042 based on a length weighted average cable to tube area ratio of 0.166 (cable area equals 0.466 in.^{2} for d_c = 0.77 inch). A more complete analysis of the full scale barrier tests produced an average value of cable drag coefficient equal to 0.0040 ranging from 0.0035 to 0.0049 for 90 data points from ten separate barrier tests.

D. Water Bleed

Tests were conducted to determine if water bleed would effectively reduce the cable drag in a water tube. It is obvious that a true drag coefficient based on the relative velocity of the cable to the water would not be affected by bleed. The apparent drag coefficient based on cable velocity and thus the cable tension would be reduced since the relative velocity of the cable to the water would be lowered. During bleed operation, the effective velocity used to determine a true drag coefficient would be equal to the cable velocity minus the peak velocity in the profile of the water bleed flow. Calculations have shown that the peak velocity of bleed flow is one and one-half to two times the average velocity based on the water tube cross-sectional area. This low Reynolds number profile of the bleed flow becomes extremely useful in reducing total cable drag because drag is a function of the square of velocity and even a small reduction in the relative velocity due to bleed flow results in a significant drag reduction for a given cable velocity. Figure 19 shows the effectiveness of bleed in the 3.83 inch tube. Bleed tests were also conducted with the 1.94 inch diameter tube and the results are presented in figure 15. A comparison of the bleed tests, figure 17, further substantiates the bleed effectiveness. These curves (figure 17) show that the apparent drag coefficient is a function also of the length to diameter ratio of the water tube. For a given tube diameter, the end pressure built up due to cable drag increases as the length is increased. The increased pressure will increase the bleed rate for a given orifice diameter which further reduces the water velocity relative to the cable.

The use of water bleed should be useful as a control parameter during operation with a piston or pistons attached to the cable. The effect of the piston increases the water pressure level ahead of it, permitting very high water flow rates with its associated drag reduction.

E. Single and Double Piston Drag

Several tests were run using both a single and double piston arrangement with the shortened water squeezer shown in figure 9. The piston geometry is shown in figure 20. The double piston combination utilized an added piston of identical geometry with twenty-five foot separation. An immediate indication from these tests was that the double piston arrangement was more stable as evidenced by the comparatively more stable recordings of the pressure and force transducers during the double piston test runs, when compared with the single piston data.

The calculated values for the single piston are shown in figure 21 where C_e is plotted versus velocity. The scatter in the data indicates that a good simulation of full scale water squeezer operation is difficult to achieve. Test runs were conducted for a comparison between pressure relieving the retrieve end of the water tube and closing it off. This comparison showed that although the arrest pressure was essentially the same, the tube thrust was reduced a small amount when the retrieve end was relieved. Subsequent tests were made with it closed off since it would give more uniform flow conditions throughout the total tube length.

The relationship between flow coefficient, C_e, and a drag coefficient, C_D, is

$$C_e = \sqrt{\frac{V_c^2}{F_p} K_p^2} \quad ; \quad C_D = \frac{F_p}{\frac{\rho}{2} A_p V_c^2}$$

then

$$F_p = \frac{V_c^2 K_p^2}{C_e^2} = C_D \frac{\rho}{2} A_p V_c^2$$

$$C_D = \left(\frac{2 K_p^2}{\rho A_p} \right) \left(\frac{1}{C_e^2} \right) \tag{4}$$

With the above relationship, piston drag coefficient was calculated for various piston-tube combinations using the average flow coefficient from figure 21. The results plotted in figure 22 also show data points from full scale tests for comparison.

A. 5/8" Standard Lay 6 x 19 I. W. R. C., O. D. = 0. 652

B. 1/2" Armoured Strand, O. D. = 0. 658

FIGURE 12: TEST CABLE SPECIMENS

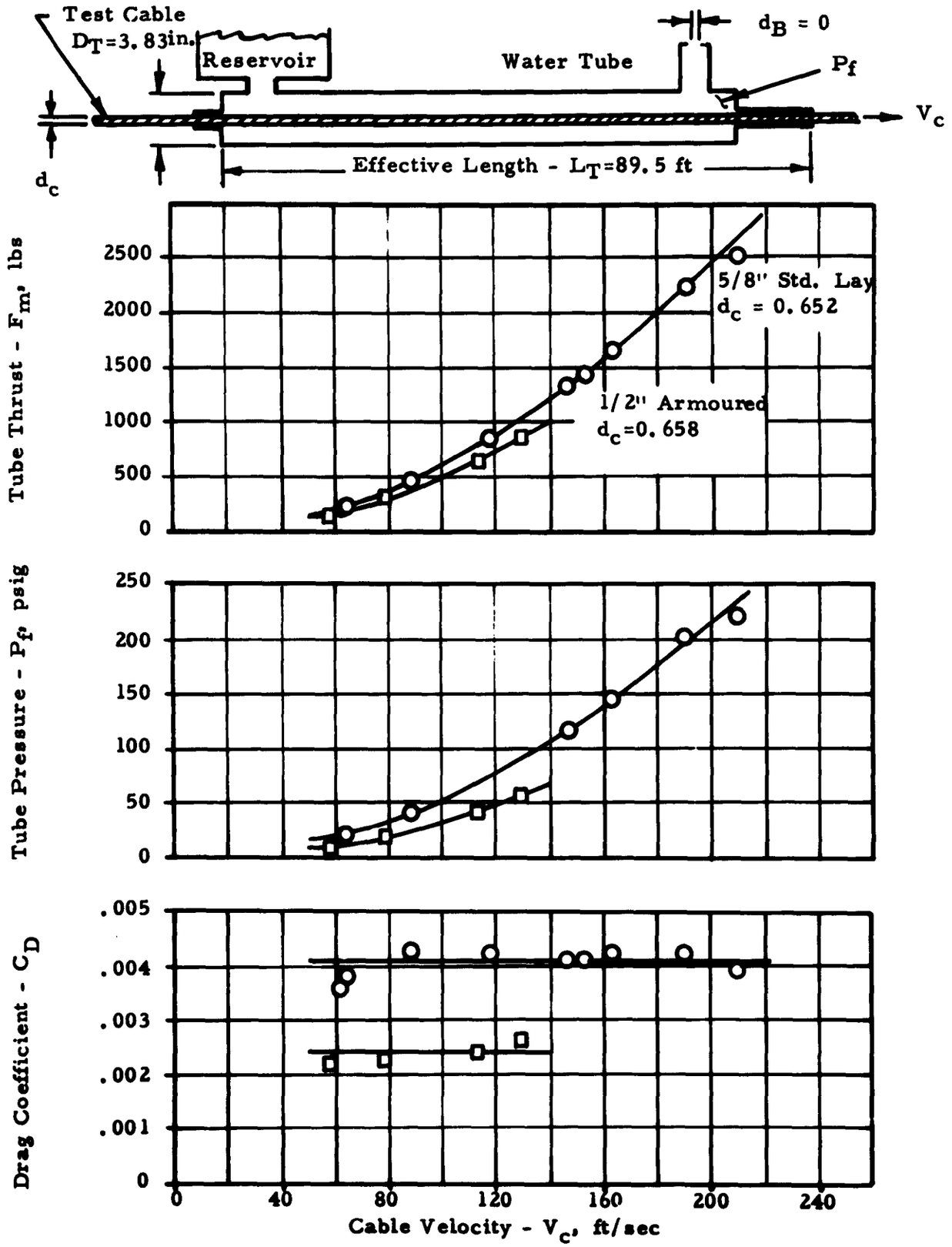

FIGURE 13: COMPARISON OF CABLE DRAG PARAMETERS VERSUS CABLE VELOCITY FOR CHANGE IN TEST CABLE GEOMETRY

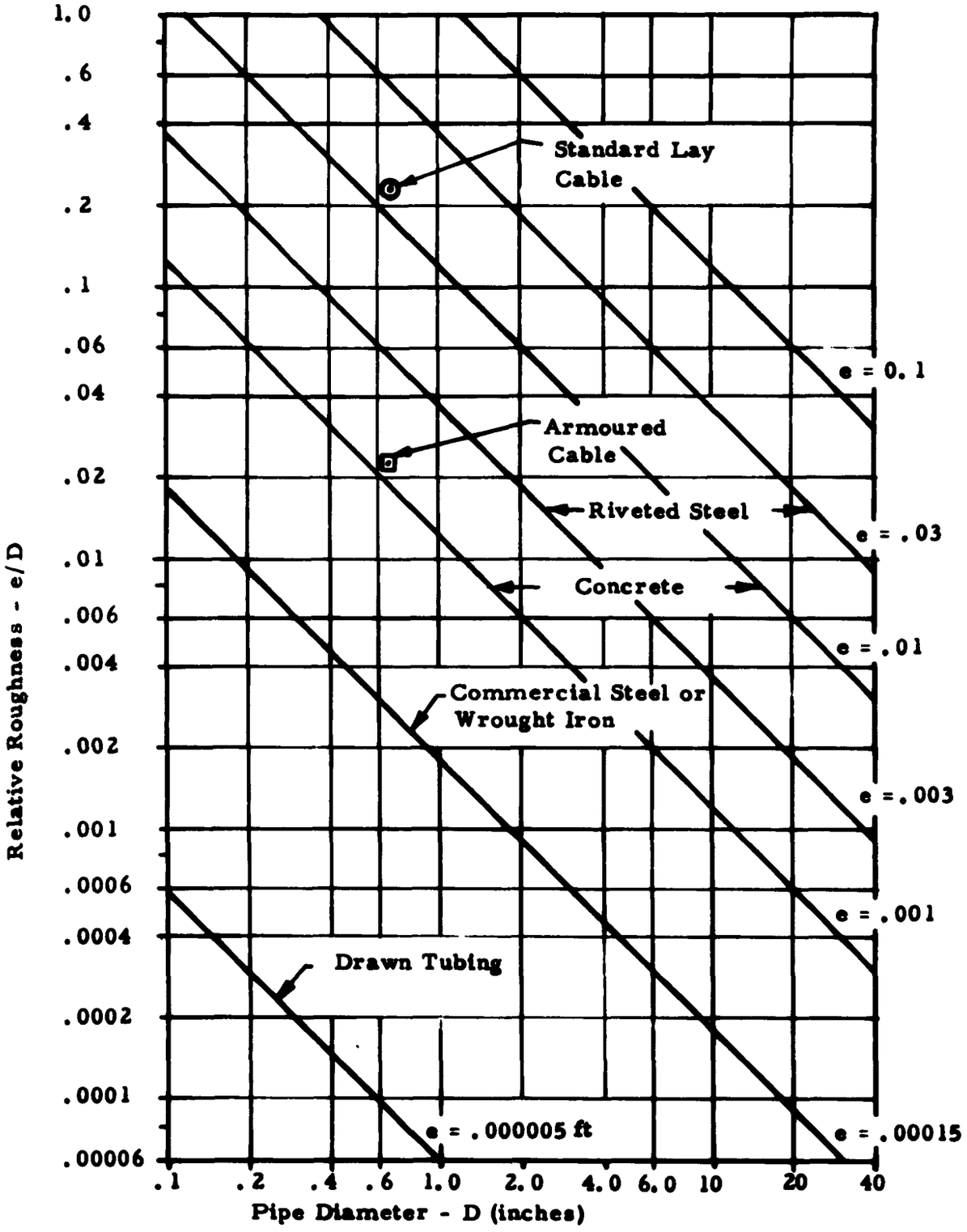

FIGURE 14: COMPARISON OF CABLE ROUGHNESS WITH OTHER MATERIALS

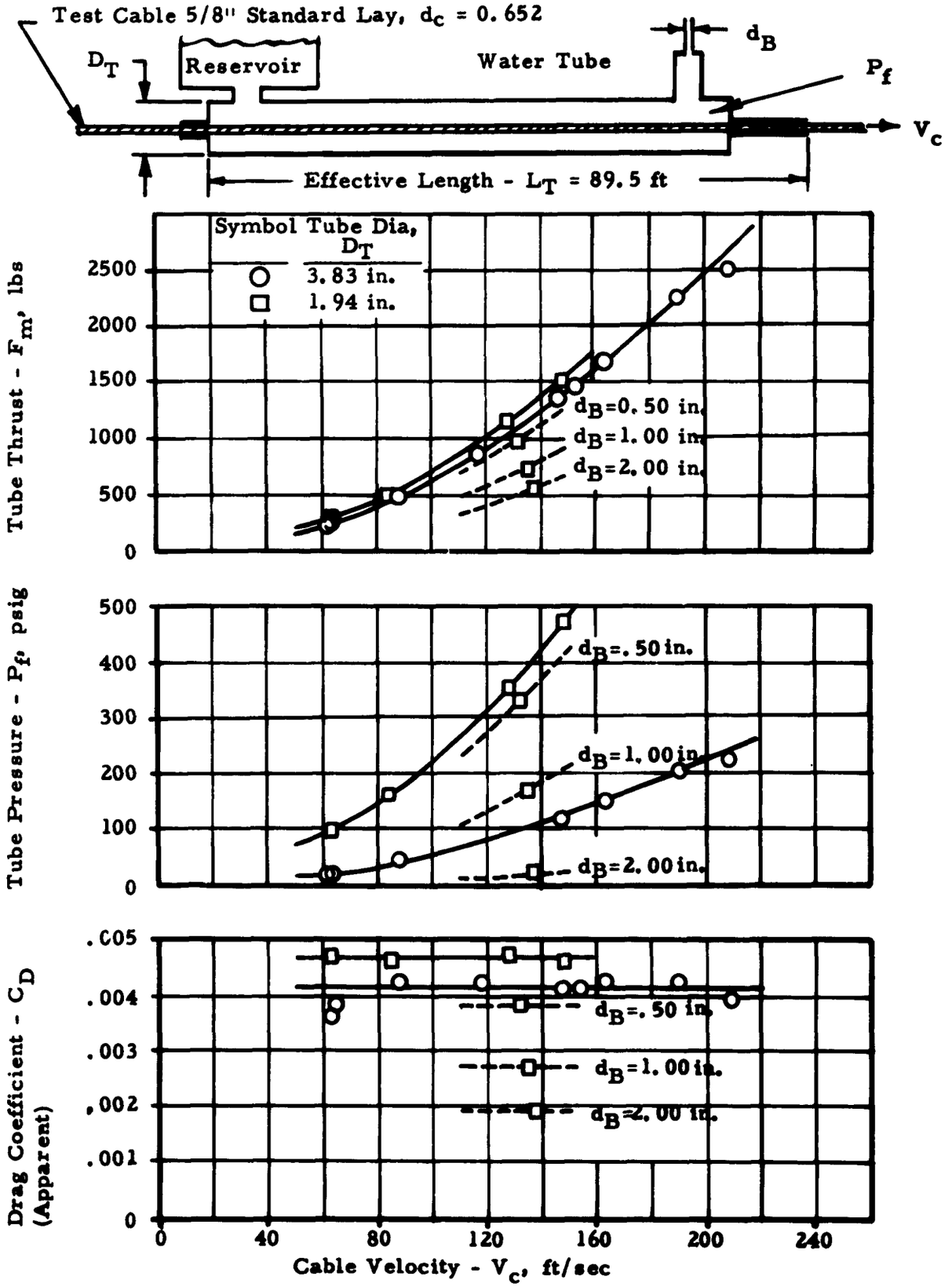

FIGURE 15: COMPARISON OF CABLE DRAG PARAMETERS AT ZERO BLEED VERSUS VELOCITY FOR CHANGE IN TUBE DIAMETER. (Dashed Curves Show Small Tube With Bleed)

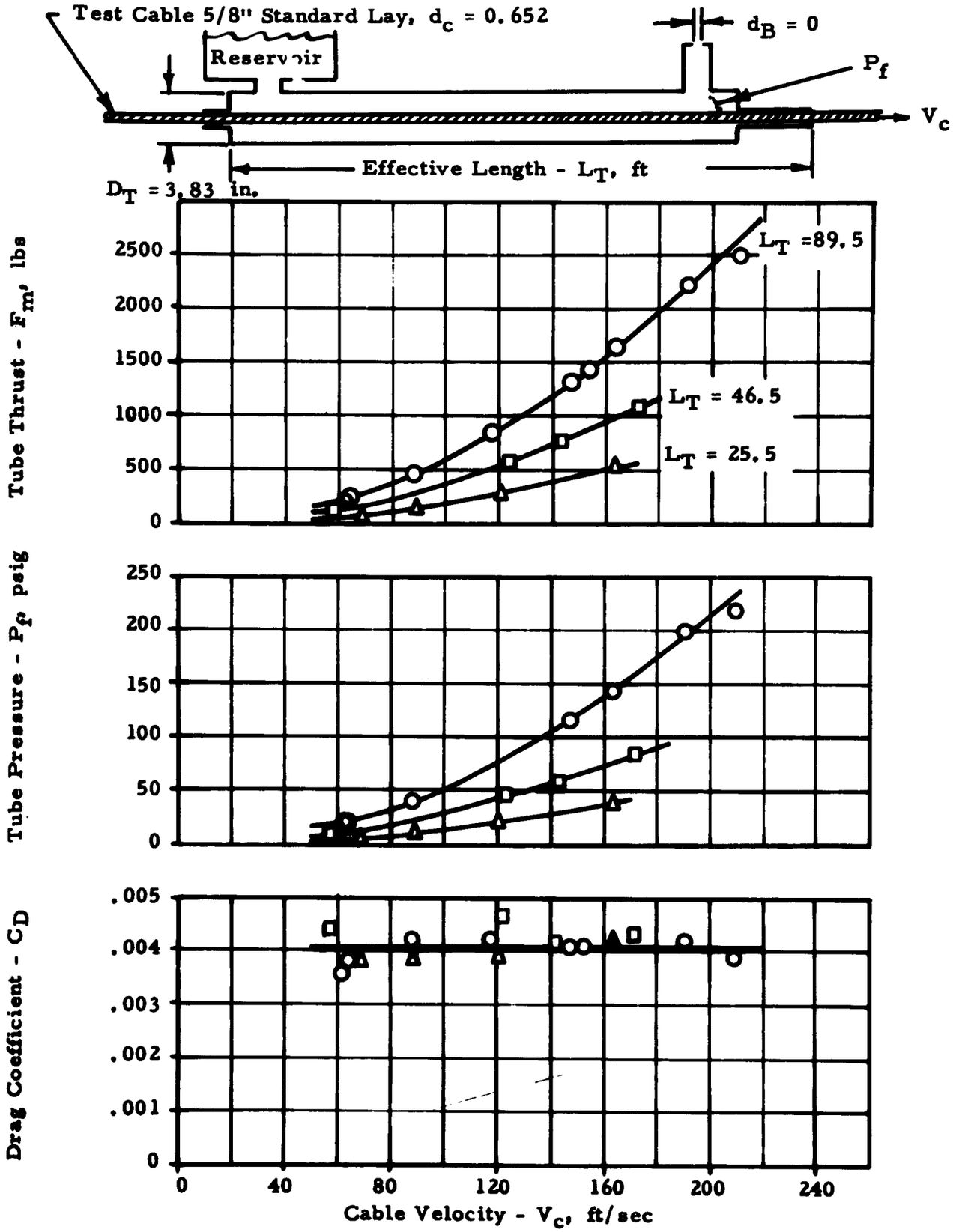

FIGURE 16: COMPARISON OF CABLE DRAG PARAMETERS VERSUS VELOCITY FOR CHANGE IN TUBE LENGTH

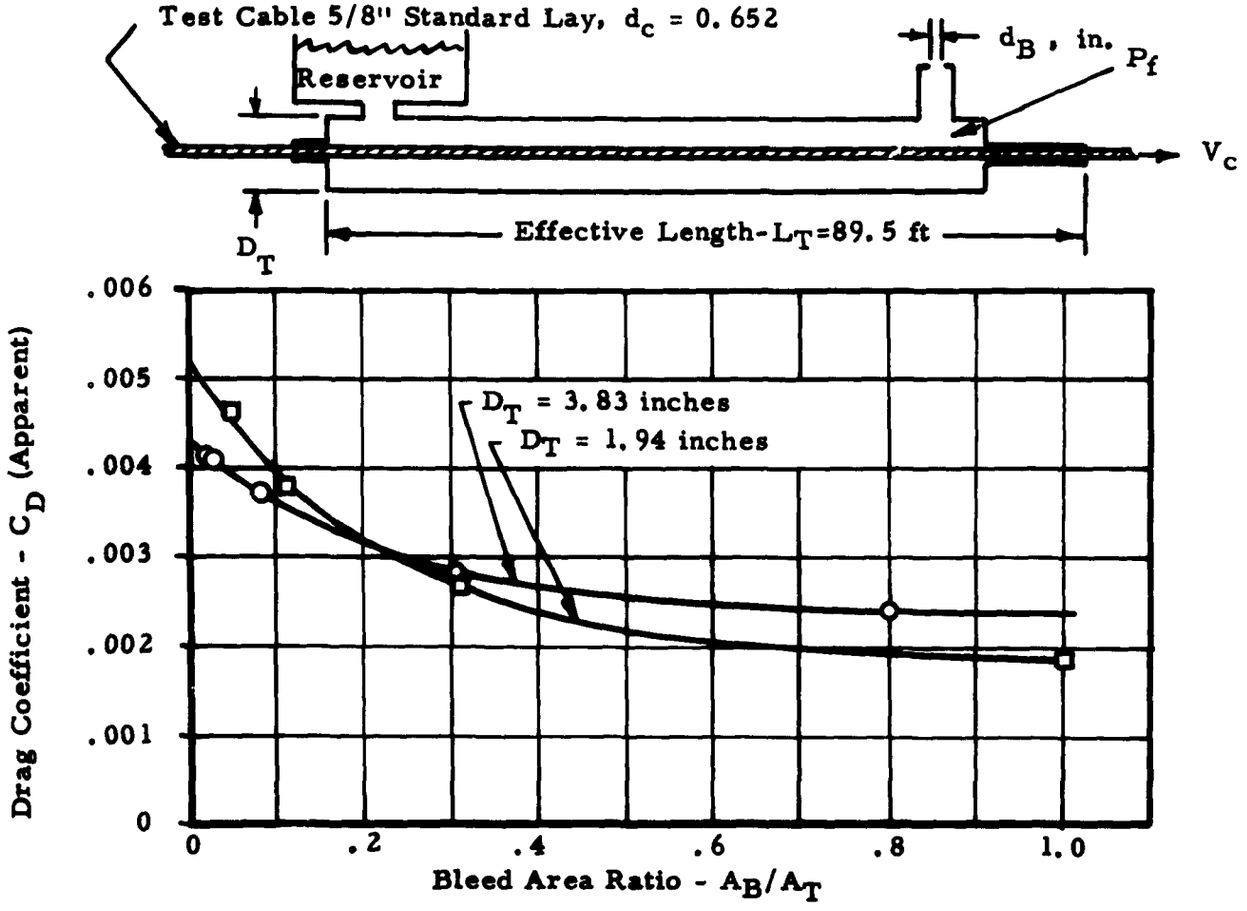

FIGURE 17: EFFECT OF BLEED AREA RATIO ON THE APPARENT DRAG COEFFICIENT

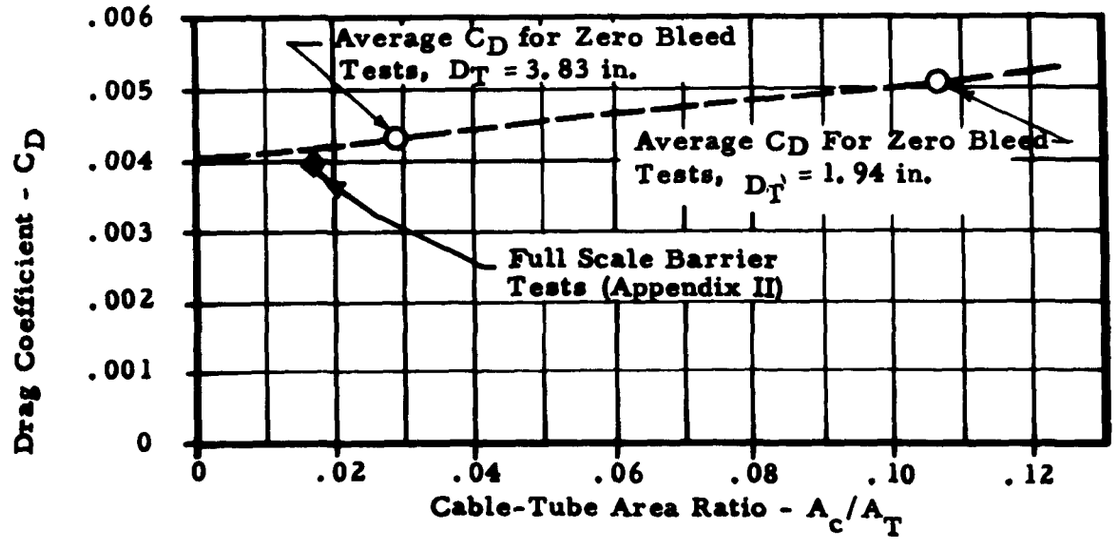

FIGURE 18: EFFECT OF CABLE-TUBE AREA RATIO ON ZERO BLEED DRAG COEFFICIENT

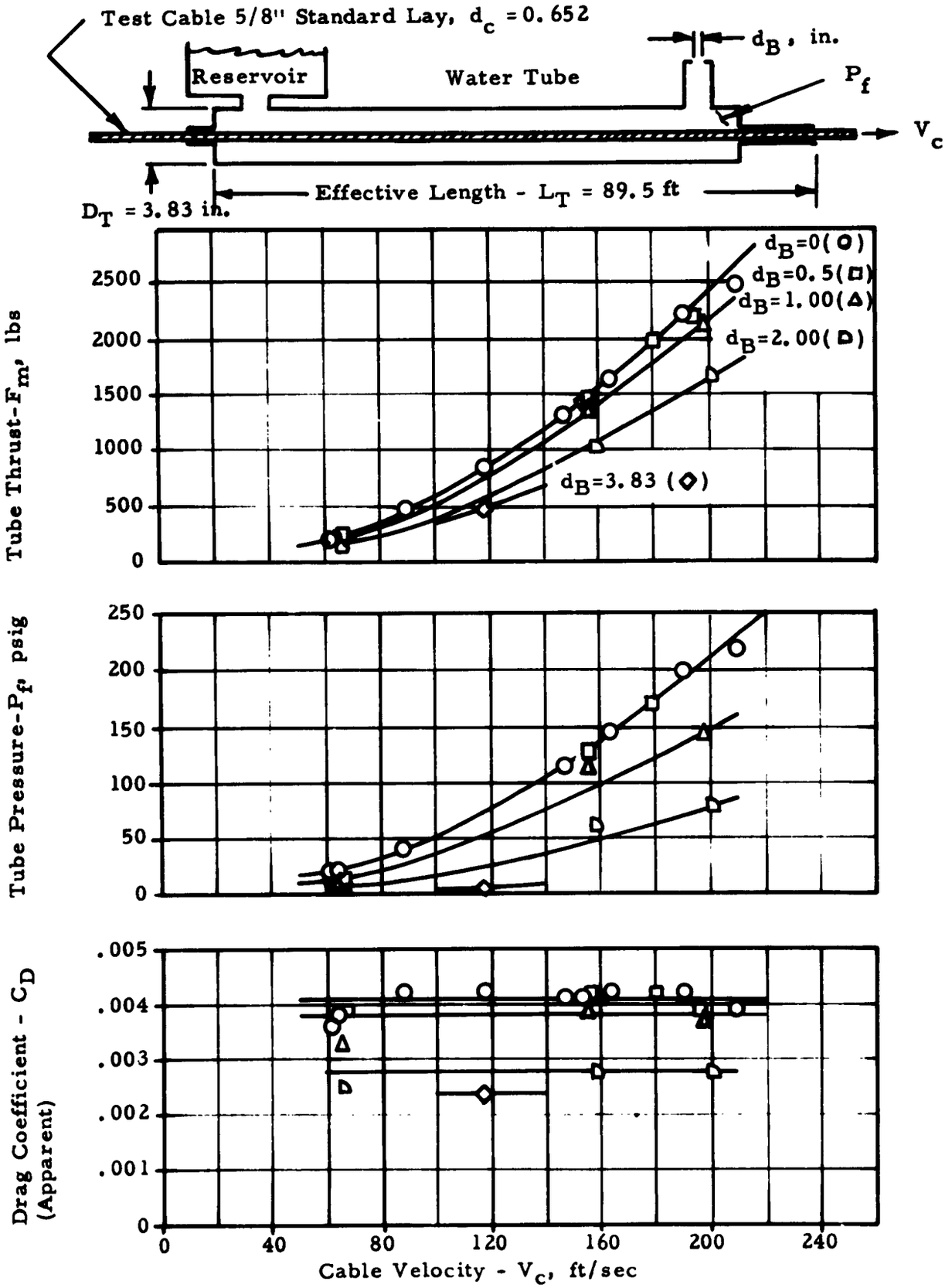

FIGURE 19: COMPARISON OF CABLE DRAG PARAMETERS VERSUS VELOCITY FOR CHANGE IN BLEED ORIFICE DIAMETER

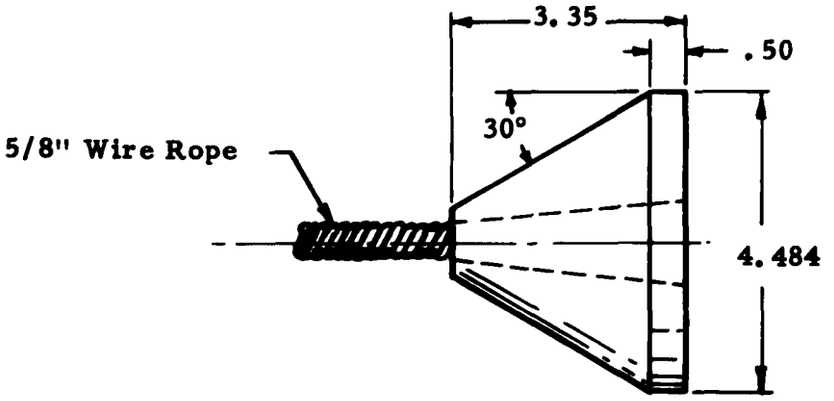

FIGURE 20: ALUMINUM PISTON GEOMETRY FOR HYDRAULIC ENERGY ABSORBER SIMULATION TESTS

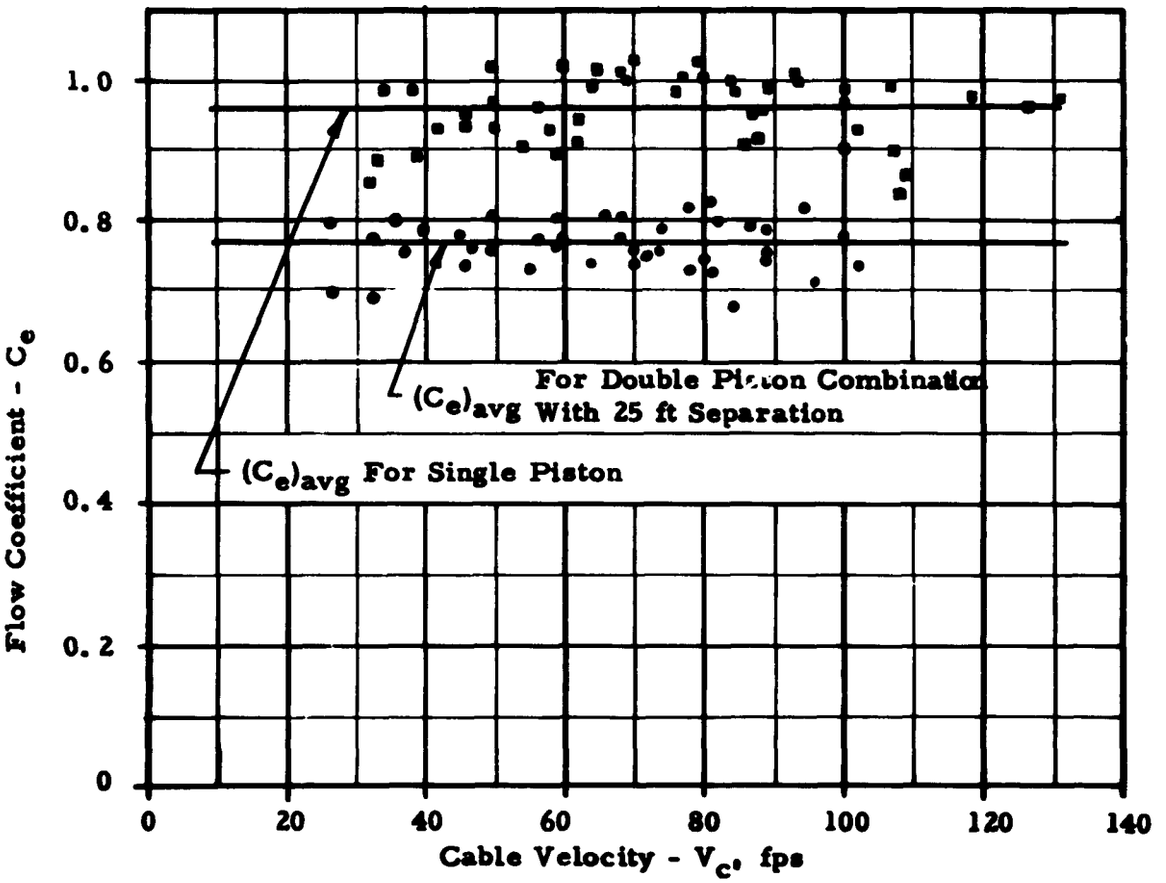

FIGURE 21: CALCULATED FLOW COEFFICIENT VERSUS CABLE VELOCITY FOR SINGLE AND DOUBLE PISTON

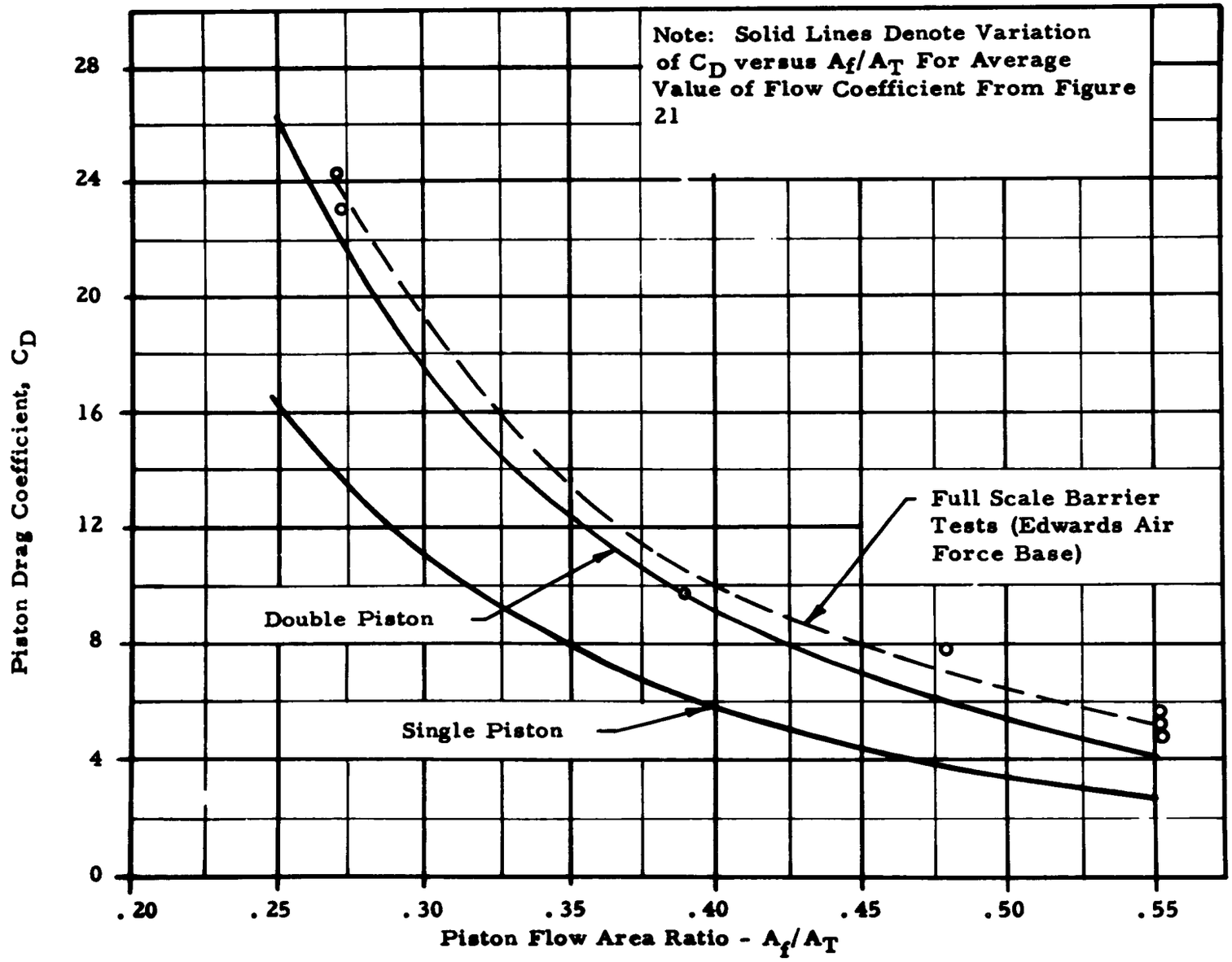

FIGURE 22: EFFECT OF PISTON FLOW AREA RATIO ON PISTON DRAG COEFFICIENT

SECTION IV

CONCLUSIONS

The results of the investigation covered by this report define many of the hydraulic energy absorber design relationships and should provide adequate information for further development.

A. Cable Drag Versus Velocity

The fact that drag coefficient was constant over the velocity range of the tests, results in a direct variation of total cable drag with the square of the cable velocity.

B. Cable Diameter Versus Tube Diameter

The cable drag coefficient was determined for a change in cable to tube area ratio. For the range investigated, a linear variation appears reasonable thus the value of $C_D = 0.004$ for $A_C/A_T = 0$ increased to $C_D = 0.005$ at $A_C/A_T = 0.1$. In terms of tube diameter for a 3/4 inch cable, $A_C/A_T = 0.1$ is equivalent to a tube diameter of 2.45 inches.

C. Cable Roughness

A comparatively smooth test cable was found to give 40 percent less drag than a standard lay cable. In practical use the drag reduction would be approximately 20 percent because an increased diameter armoured cable would be necessary for equivalent strength. Non-linear interpolation for drag correction due to cable roughness may be made by referring to friction factor curves in any fluid mechanics handbook.

D. Cable Drag Versus Cable Length

The cable drag coefficient was appropriately based on the wetted surface area of the cable. Tests on three different water tube lengths indicated no variance of the drag coefficient. The test results show that total cable drag as well as the pressure rise due to cable drag was directly proportional to the water tube length for a constant diameter tube. Full scale barrier test results substantiated this relationship.

E. Water Bleed For Cable Drag Reduction

The effect of water bleed was found to significantly reduce total cable drag. The tests on the 3.83 inch water tube showed a reduction in drag

coefficient from 0.0042 at zero bleed to a value of 0.0026 for a bleed area ratio, $A_B/A_T = 0.5$. The tests with the smaller water tube ($D_T = 1.94$) showed an even greater bleed effect. The zero bleed drag coefficient of 0.0052 was reduced to 0.0022 at $A_B/A_T = 0.5$. The greater effectiveness in this case indicates that as the length to diameter ratio of the water tube was increased, the effect of bleeding from a given sized orifice results in a more significant decrease in cable drag.

F. Piston Drag Versus Orifice Area

Tests on a shortened hydraulic energy absorber showed that a flow coefficient, calculated using a velocity of approach correction, was approximately constant with velocity and independent of changes in tube schedule. An average value of $C_e = 0.97$ was determined for the single piston. The average flow coefficient value for the double piston combination was found to be 0.77. Comparison of these results show that since piston drag is inversely proportional to the square of the flow coefficient, the effect of the added piston increased drag by 59 percent.

Determination of Cable Surface Roughness

Determination of the Reynolds number shows that the water flow adjacent to the test cable is turbulent, thus the viscous shear of the fluid occurs in a relatively thin layer close to the cable surface. The sketch below illustrates typical turbulent flow conditions.

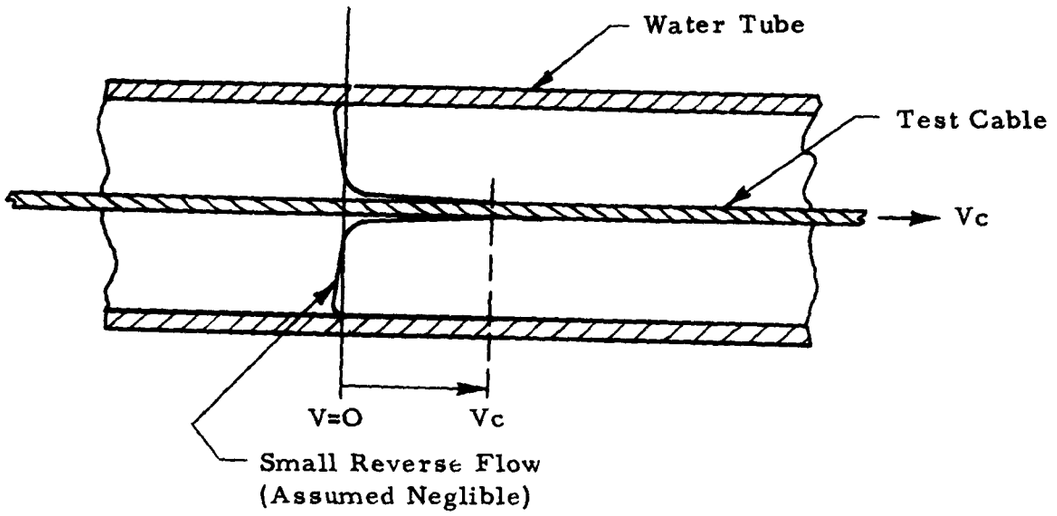

At Reynold's number above 10^4 (turbulent regime) in pipe flow there is a similar distribution of shear forces, in that they exist only in a thin layer close to the pipe wall - illustrated below.

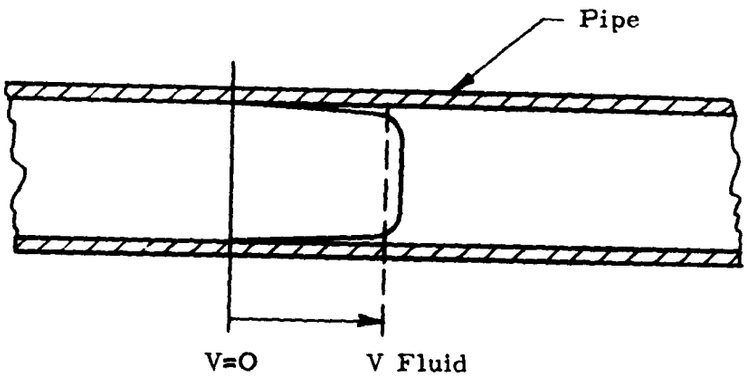

The magnitude of the shear forces in both cases must be a function of velocity and the surface roughness of the fluid boundaries. A measurement of the shear forces at a given velocity should then be a valid comparison of the surface roughness. Consider water flow at the same velocity as the test cable in a pipe of the same diameter as the test cable, and of equivalent roughness. The determination of a friction factor for this flow condition will then be a measure of roughness. Extensive study has been given to this type of pipe flow problem. An analysis by R.C. Binder* based on the work of Karman, Nikuradse, Prandtl and others gives the following solution:

Let "h' equal the head loss in the pipe length "ℓ". The friction factor "f" is then

$$f = \frac{h}{\frac{\ell}{D}\ \frac{V^2}{2g}} \qquad \text{(I-1)}$$

where: D = pipe diameter

$\frac{V^2}{2g}$ = velocity head

Roughness measurement is based on artifically but measureable roughened pipes. The mean diameter, e, of the sand grains used to coat the pipe walls is arbitrarily called the absolute roughness. The dimensionless ratio, e/D, is termed the relative roughness.

Calculation of the Reynold's number for cable velocities above 10 feet per second classifies this flow as in the rough pipe zone where the roughness and the friction factor are related by:

$$\frac{1}{\sqrt{f}} = 1.74 - 2 \log \left(\frac{2e}{D}\right) \qquad \text{(I-2)}$$

Example: Standard Lay Cable, d_c = .652

Cable Velocity, V_c = 150 fps

Tube End Pressure, P_f = 121 psig

* Binder, R.C., Fluid Mechanics, Second Edition, Prentice-Hall, Inc., New York, N.Y.

Tube Length, $L_T = 89.5$ ft

Tube Diameter, $D_T = 3.83$ in.

For analogous pipe flow:

Pipe Diameter, $D \equiv d_C$

Pipe Length, $\ell \equiv L_T$

Flow Velocity, $V \equiv V_C$

Head Loss, $h \equiv P_f \times \frac{A_T}{A_C}$

Then from equation (1)

$$f = \frac{121 \times 2.309 \left(\frac{11.46}{0.0334}\right)}{\left(\frac{89.5 \times 12}{0.652}\right) \frac{(150)^2}{2 \times 32.2}} = 0.167$$

Using this value in Equation (2)

$$\frac{1}{\sqrt{0.167}} = 1.74 - 2 \log \left(2 \frac{e}{D}\right)$$

$$\frac{e}{D} = 0.222; \qquad e = 0.0120 \text{ ft}$$

For the case of the armoured cable, similar calculations show

$$f = 0.103; \quad \frac{e}{D} = 0.0211; \quad e = 0.0011 \text{ ft}$$

It should be noted that interpolation for cable roughness calculations must be made with caution because of the non-linear relationship of "f" with (e/D) shown by equation (I-2).

APPENDIX II

A. Cable Drag and Pressure Distribution In A Tapered Or Stepped Tube

It was shown in the tests that the cable drag in a constant diameter tube is equal to the pressure build-up times the tube cross-sectional area. In a stepped tube the pressure distribution obviously depends on the tube areas involved. Consider a stepped tube made up of three tubes of lengths ℓ_1, ℓ_2, and ℓ_3, illustrated in figure 23. Assume that the difference in tube diameters is small enough so that the difference in their respective drag coefficients is negligible. For a given velocity, V_C, the total cable drag force, D_C, is then independent of the tube areas. If the total tube length was of constant diameter tubing with area equal to A_1 then

$$D_C = P_1 A_1 \tag{II-1}$$

Similarly if the tubing was of diameters D_2 or D_3:

$$D_C = P_2 A_2 = P_3 A_3 \tag{II-2}$$

The pressure distribution for the stepped schedule illustrated becomes obvious. For X equal 0 to ℓ_1 the pressure increase is identical to that when tubing D_1 was considered constant throughout the total length. The distribution from $X = \ell_1$ to $X = \ell_1 + \ell_2$ has merely an increased rate of pressure build-up from the point $X = \ell_1$, parallel to P_2. Through the last tube section the rate of pressure increase is parallel to P_3.

It is interesting to note that the final end pressure P_A at $X = \ell$ may be obtained by a different method. Since the cable drag coefficient for the three different tube sections was assumed constant, there is an average tube size that will give a straight line pressure distribution from zero at X = 0 to P_A at $X = \ell$. The area of this hypothetical tube is

$$A_i = D_C / P_A \tag{II-3}$$

It can be shown that A_i is actually a length weighted average tube size thus

$$A_i = \frac{A_1 \ell_1 + A_2 \ell_2 + A_3 \ell_3}{\ell_1 + \ell_2 + \ell_3} \qquad \text{(II-4)}$$

B. Full Scale Barrier Tests, Cable Drag

Oscillograph data from full scale barrier tests at Edwards Air Force Base were analyzed to obtain comparative results for the controlled tests at Research, Incorporated. The illustration, figure 24, shows the scheduling of the water squeezer tube section. Pertinent information concerning the test operation is listed in the notes. The determination of cable drag was accomplished by examining the data traces during the time interval after the cable was brought up to velocity by the engagement, but before the pistons entered the water-filled tube sections. Examination of the traces at several points during this interval gave the data tabulated in the Table III.

Velocity taken from a count of sheave revolutions was plotted versus time in figure 25. The variation shown by the data points is obviously not representative of an average velocity seen by 650 feet of wetted cable. A straight line variation through these points (dashed lines) was considered more realistic. It was during this part of the analysis that an original assumption of 3.93 ft per mark on the cable travel transducer was found to be in error. A marked change in pressure due to the passing of the second piston was correlated with a count of the sheave revolutions between two pressure transducers at a known distance apart. Analysis of this information showed cable travel to be 3.72 feet per mark, or a reduction of 5.35 percent in the calculated velocity based on 3.93 feet per mark. The solid line on figure 25 then represents the corrected velocity versus time based on 3.72 feet per mark. The slope of this curve gives the average deceleration of 21.2 feet/second^2. To obtain drag coefficient, the deceleration force of the mass upstream (towards pistons) of the tensiometer was added to the tensiometer measurement. Drag coefficient was then calculated from the equation below and listed in the tabulation Table III.

$$C_D = \frac{D_c}{\rho/2 \, A \, V_c^{\,2}} \qquad \text{(II-5)}$$

where D_C = cable tension measurement plus deceleration force, lbs.

ρ = water density, lbs sec^2/ft^4

A = wetted cable surface area, ft^2

V_C = cable velocity, ft/sec

The pressure distribution was analyzed for several data points according to the method outlined in Part A. A tabulation of this distribution is given in Table IV. Two typical distributions were plotted along with the measured transducer pressure, figure 26. The excellent correlation of the end pressure (transducer No. 5) illustrates the compatibility of this measured pressure with the measurement of cable tension, since the assumed pressure distribution is a function of cable drag. The measured data points also show the effect of tube diameter on drag coefficient by reason that the calculated distribution assumes a constant drag coefficient which is valid for predicting the end pressure (No. 5). The dashed line shown in the figure represents the distribution of pressure using the hypothetical tube method. Using equations (II-3) and(II-4) the length-weighted average tube area was found to be 28.00 $in.^2$. This figure can be useful for quickly evaluating the correlation between tube end pressure and the measured cable drag.

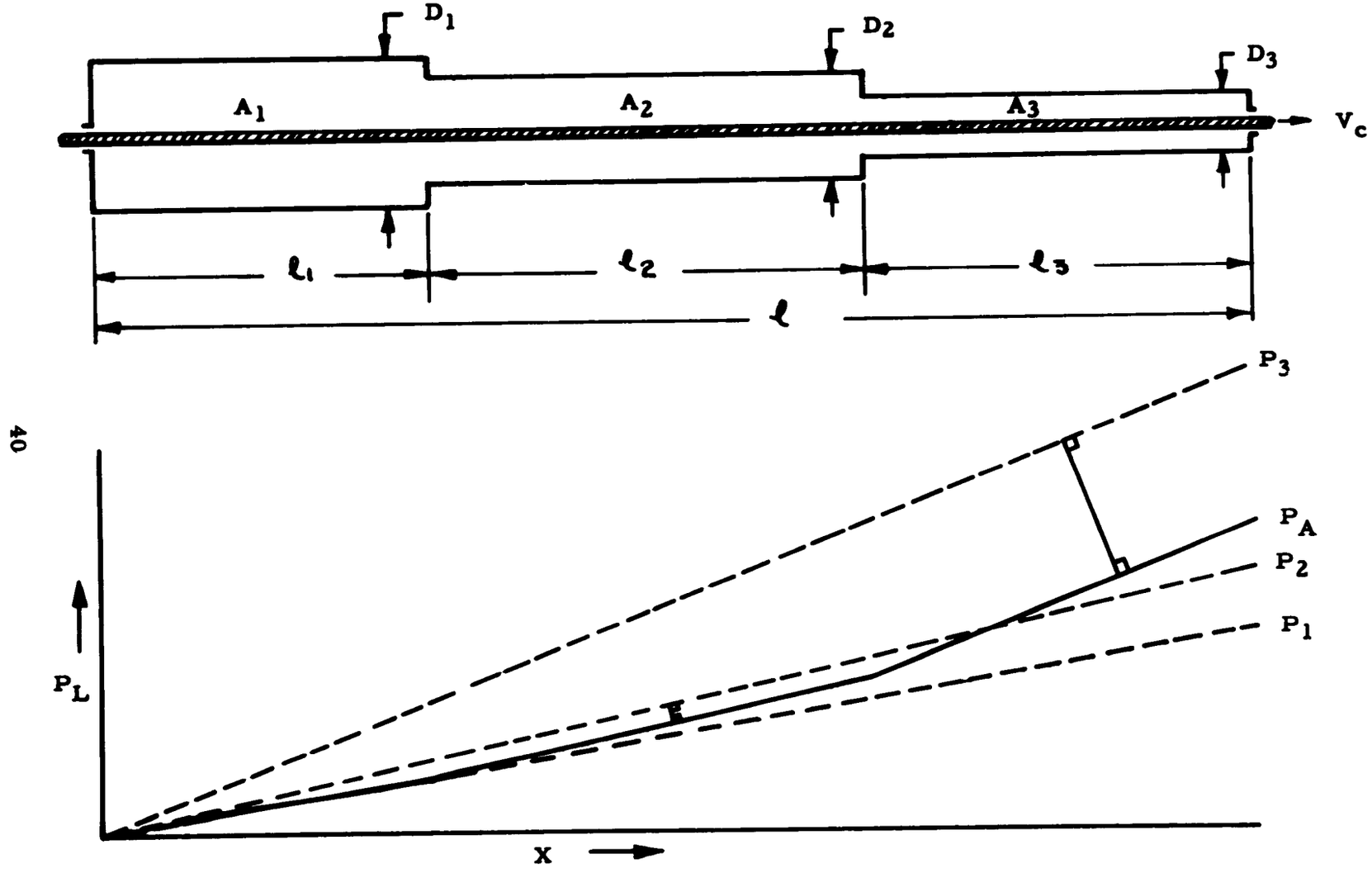

FIGURE 23: ILLUSTRATION OF PRESSURE DISTRIBUTION DUE TO CABLE DRAG IN STEPPED TUBE

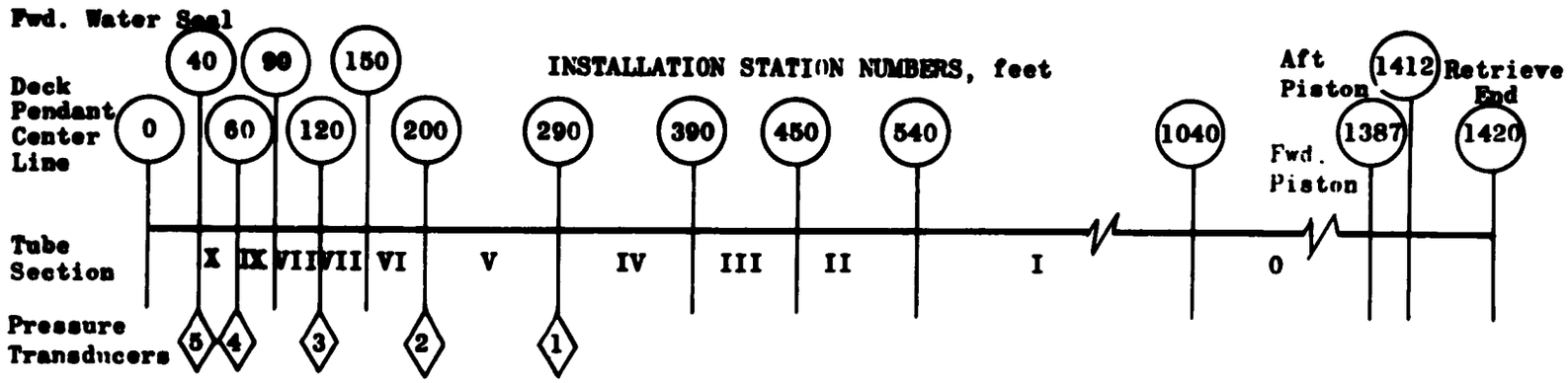

1. Tube Schedule:

Section	I.D., inches	Length, feet
0	5.625	380
I	7.250	500
II	7.000	90
III	6.500	60
IV	6.000	100
V	5.500	90
VI	5.250	50
VII	5.125	30
VIII	5.000	30
IX	4.875	30
X	4.750	20

Section 0 3/16 inch wall thickness
Sections I-X 3/8 inch wall thickness

2. Pistons: Forward and Aft
4 11/16 inches O.D., spaced 25 feet apart
Steel, weight 14.5 pounds per piston

3. Deck Sheaves: 375 feet center to center.

4. Cables:
6 x 19 I.W.R.C. steel cable, 3/4 inch diameter
Deck Pendant 300 ± 1 foot
Purchase cable 1425 ± 1 foot
Connecting cable 25 ± 1 foot

5. Retrieve Line: 9/16 inch diameter nylon rope

6. Tube Slope:

Station	Datum, inches
40	-12.00
230	-24.00
680	0.00
1015	+18.00
1040	+24.00

7. Water Capacity: Normal fill 1065 gallons.
Fill to Station 690

8. Water dip in aft end of tube, 6 inch drop in section approximately 75 feet long. Pistons initially in dry tube aft of water dip.

FIGURE 24: ILLUSTRATION OF FULL SCALE WATER SQUEEZER INSTALLATION

Position No.	140	160	180	200	220	240	260	280	300	350
Cable Travel	275	314	354	393	432	472	510	550	589	687
Time, seconds	1.644	1.837	2.030	2.229	2.430	2.634	2.845	3.060	3.284	3.870
Velocity, fps (Tachometer)	207	207	200	197	197	189	180	180	172	164
Velocity, fps (Corrected)	199.5	195.2	191.0	187.0	182.7	178.3	173.7	169.1	164.3	154.0
Force, lb	15,900	16,300	15,400	14,200	14,200	13,900	13,380	12,700	11,900	10,830
Pressure, ⟨1⟩ psig	275	275	255	265	255	275	235	214	214	204
Pressure, ⟨2⟩ psig	372	370	350	350	330	360	310	290	280	250
Pressure, ⟨3⟩ psig	437	437	410	410	410	418	362	362	326	288
Pressure, ⟨4⟩ psig	530	530	498	488	467	488	427	396	396	346
Pressure, ⟨5⟩ psig	610	587	574	557	523	557	475	457	457	392
Deceleration Force, lb	720	700	680	660	640	620	590	570	540	470
Cable Drag (Constant V)	16,220	17,000	16,080	16,060	14,840	14,520	13,970	13,270	12,440	11,300
$(C_D)_C = 2D_C/\rho A_C V_C^2$	.00329	.00352	.00347	.00362	.00351	.00360	.00365	.00365	.00364	.00375

TABLE III: TABULATION OF OSCILLOGRAPH DATA FROM TYPICAL FULL SCALE BARRIER TEST (Edwards Air Force Base - BAK-6 Test No. 148 - Left Side)

Position No.	460	480	500	520	540	630	640	665
Cable Travel, ft	904	943	982	1020	1060	1172	1192	1238
Time, seconds	5.374	5.690	6.033	6.396	6.787	8.810	9.143	10.15
Velocity, ft/sec (Tachometer)	127	119	113	105	95	---	---	---
Velocity, ft/sec (Corrected)	102.2	113.7	106.4	98.6	90.0	59.0	54.0	42.0
Force, lb	12,300	11,230	10,170	10,830	10,830	9,500	8,300	7,500
Pressure, psig ◇1	418	357	306	368	408	---	---	---
Pressure, psig ◇2	460	400	340	420	410	380	330	---
Pressure, psig ◇3	455	409	344	446	409	362	306	325
Pressure, psig ◇4	427	437	366	498	437	376	325	325
Pressure, psig ◇5	436	480	392	501	457	382	327	327
Deceleration Force, lb	320	290	270	240	210	115	107	72
Cable Drag + Piston Drag (Constant V)	12,620	11,520	10,440	11,070	11,040	9,615	8,402	7,572
$D_C = (C_D)_C A_C V_C^2 \rho/2$	4,960	4,150	3,350	2,620	1,960	430	319	123
Piston Drag (D_p)	7,660	7,370	7,090	8,450	9,080	9,185	8,083	7,449
$(C_D)_P = 2D_p/A_p V_C^2 \rho$	1.65	5.00	5.49	7.63	9.83	23.1	24.3	37.0

TABLE III (Cont): TABULATION OF OSCILLOGRAPH DATA FROM TYPICAL FULL SCALE BARRIER TEST

Pressure Transducer Position		⑤	④		③		②	①			
Tube Length, ft		20	30	30	30	50	90	100	60	90	150
$\Delta D_c/D_c$		.0308	.0461	.0461	.0461	.0768	.1388	.1536	.0022	.1388	.2307
A_T		17.67	18.62	19.58	20.58	21.60	23.71	28.22	33.13	38.43	41.23
$\Delta P/D_c = \Delta D_c/D_c A_T$		.00174	.00247	.00235	.00224	.00355	.00586	.00544	.00279	.00361	.00560
Oscillograph Data Position											
160	ΔP_L	29.6	42.0	40.0	38.1	60.4	99.5	92.5	47.4	61.3	95.3
	P_L	606.1	576.5	534.5	494.5	456.4	396.0	296.5	204.0	156.6	95.3
	P_m	587	530		437		370	275			
180		28.0	39.7	37.8	36.0	57.1	94.2	87.6	44.9	58.0	90.1
		573.4	545.4	505.7	467.9	431.9	374.8	280.6	193.0	148.1	90.1
		574	498		410		350	255			
200		28.0	39.7	37.8	36.0	57.1	94.2	87.6	44.9	58.0	90.1
		573.4	545.4	505.7	467.9	431.9	374.8	280.6	193.0	148.1	90.1
		557	488		410		350	265			
220		25.9	36.7	34.9	33.2	52.7	87.0	80.8	41.4	53.6	83.1
		529.3	503.4	466.7	431.8	398.6	345.9	258.9	178.1	136.7	83.1
		523	467		410		330	255			
240		25.3	35.9	34.2	32.5	51.6	85.0	79.0	40.4	52.4	81.2
		517.5	492.2	456.3	422.1	389.6	338.0	253.0	174.0	133.6	81.2
		557	488		418		360	225			
260		24.3	34.5	32.8	31.3	49.6	81.8	76.0	39.0	50.4	78.2
		497.9	473.6	439.1	406.3	375.0	325.4	243.6	167.6	128.6	78.2
		475	427		362		310	235			
280		23.1	32.8	31.2	29.7	47.2	77.7	72.2	37.0	47.9	74.3
		473.1	450.0	417.2	386.0	356.3	309.1	231.4	159.2	122.2	74.3
		457	396		362		290	214			
300		21.7	30.7	29.2	27.9	44.2	72.9	67.7	34.7	44.9	69.7
		443.6	421.9	391.2	362.0	334.1	280.9	217.0	149.3	114.6	69.7
		457	396		326		280	214			
350		19.7	27.9	26.6	25.3	40.2	66.2	61.5	31.5	40.8	63.3
		403.0	383.3	355.4	328.8	303.5	263.3	197.1	135.6	104.1	63.3
		392	346		288		250	204			

TABLE IV: TABULATION OF PRESSURE DISTRIBUTION FOR FULL SCALE BARRIER TEST

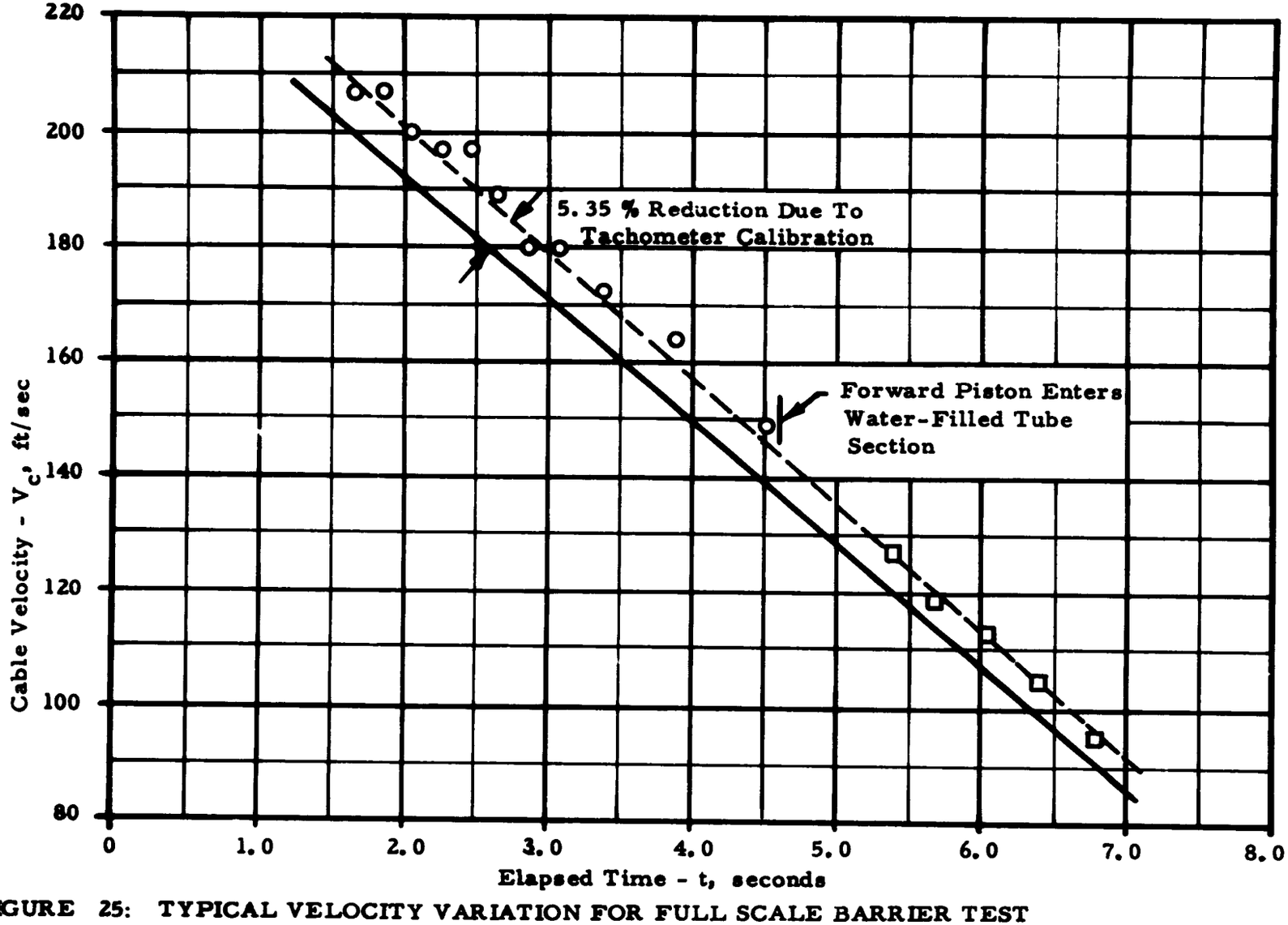

FIGURE 25: TYPICAL VELOCITY VARIATION FOR FULL SCALE BARRIER TEST (Edwards Air Force Base - BAK-6, No. 148 Left)

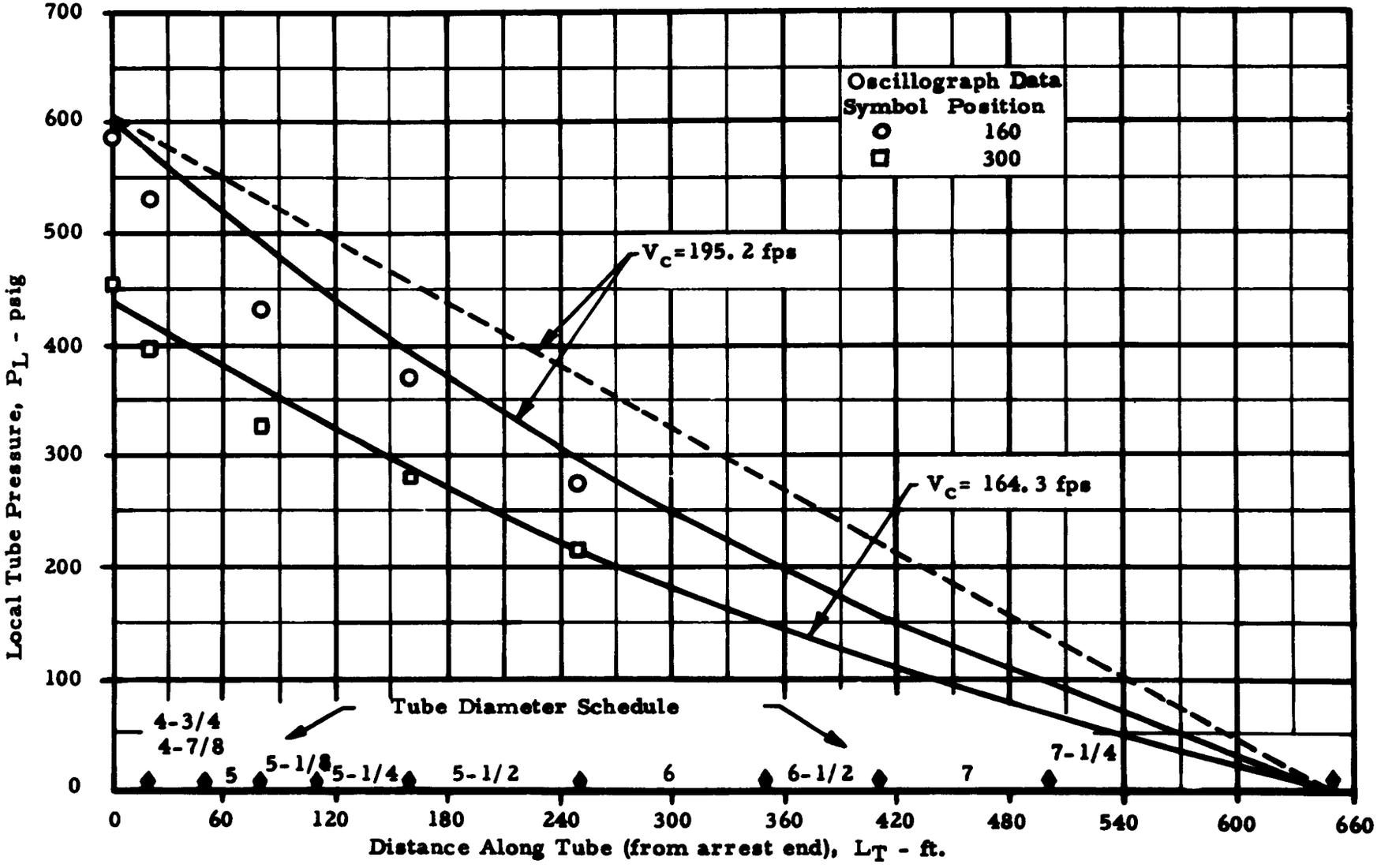

FIGURE 26: COMPARISON OF PREDICTED DISTRIBUTION WITH MEASURED VALUES FROM FULL SCALE BARRIER TEST (Edwards Air Force Base - BAK-6, No. 148, Left)

* U.S. GOVERNMENT PRINTING OFFICE: 1961 O - 605582